



# Measuring evapotranspiration on an eroded cropland by an automated and mobile chamber system: gap filling strategies and impact of soil type and topsoil removal

5 Adrian Dahlmann<sup>1</sup>, Mathias Hoffmann<sup>1</sup>, Gernot Verch<sup>2</sup>, Marten Schmidt<sup>1</sup>, Michael Sommer<sup>3,4</sup>, Jürgen Augustin<sup>1</sup>, Maren Dubbert<sup>1</sup>

<sup>1</sup>Isotope Biogeochemistry and Gas Fluxes, Leibniz Centre for Agricultural Landscape Research, Müncheberg, 15374, Germany

<sup>2</sup>Experimental Station Dedelow, Leibniz Centre for Agricultural and Landscape Research, Prenzlau, 17291, Germany

10 <sup>3</sup>Landscape Pedology, Leibniz Centre for Agricultural Landscape Research, Müncheberg, 15374, Germany

<sup>4</sup>Institute of Geography and Environmental Science, University of Potsdam, 14476, Potsdam, Germany

*Correspondence to:* Adrian Dahlmann (adrian.dahlmann@zalf.de)

**Abstract.** In light of ongoing global climate crisis and related increases in extreme hydrological events, it is increasingly crucial to assess ecosystem resilience and - in agricultural systems - to ensure sustainable management and food security. For that, comprehensive understanding of ecosystem water cycle budgets and spatio-temporal dynamics are indispensable. Evapotranspiration (ET) plays a pivotal role returning up to 90 % of ingoing precipitation back to the atmosphere. Here, we studied impacts of soil types and management on an agroecosystems water budgets and agronomic water use efficiencies (WUE<sub>agro</sub>). To do so, a plot experiment with winter rye (September 17, 2020 to June 30, 2021) was conducted at an eroded cropland which is located in the hilly and dry ground moraine landscape of the Uckermark region in NE Germany. Along the experimental plot (110 m x 16 m), a gantry crane mounted mobile and automated two chamber system (FluxCrane as part of the AgroFlux platform within the CarboZALF-D research site) was used to continuously determine evapotranspiration for the first time. Three soil types representing the full soil erosion gradient related to the hummocky ground moraine landscape (extremely eroded: Calcaric Regosol, strongly eroded: Nudiargic Luvisol, non-eroded: Calcic Luvisol) and additional soil manipulation (topsoil removal and subsoil admixture) were investigated (randomized block design, 3 replicates per treatment). Five different gap-filling approaches were used and compared in light of their potential for reliable water budgets over the entire crop growth period as well as reproduce short-term (day-to-day, diurnal) water flux dynamics. The best calibration performance was achieved with approaches based on machine learning, such as support vector machine (SVM) and artificial neural networks (with Bayesian regularization; ANN\_BR), while especially SVM yielded in best predictions of measured ET during validation. We found significant differences in dry biomass (DM) and minor in evapotranspiration between soil types, resulting in different water use efficiencies (WUE<sub>agro</sub>). The Calcaric Regosol (extremely eroded) shows a maximum of around 37% lower evapotranspiration and a maximum of around 52% lower water use efficiency (WUE<sub>agro</sub>) compared to the non-eroded Calcic Luvisol. The key period contributing to ~ 70% of overall ET of the entire growth period was from April until harvest, however



35 differences in the overall ET budget ( $ET_{sum}$ ) between soil types and manipulation resulted predominantly from small long-term differences between the treatments over the entire growth period.

## 1 Introduction

More than 70% of the global ice-free land area is directly influenced by humans in distinct ways (Shukla et al., 2019). In fact, only 12% of the world's land area is suitable for food and fiber production due to its highly productive soils, 65% of which are located in temperate and Mediterranean climatic zones and only 35% in tropical ones (Blum, 2013). Due to a still growing human population paired with the ongoing climate crisis, much of this land is already in use worldwide to ensure food security. Additionally, worldwide land area is largely affected by soil degradation (Jie et al., 2002). According to the European Union, agriculture is closely related to soil degradation, since at least six degradation processes (e.g. erosion or compaction) are associated with it (Louwagie et al., 2011). In hummocky landscapes, erosion and associated topsoil removal caused by different elements (e.g. wind, water or tillage) affects the fertility of field crops (Bakker et al. 2007; Biggelaar et al. 2003). Moreover, the global climate crisis, for example, is affecting the amount and spatio-temporal distribution of precipitation worldwide, leading to more frequent and stronger events in high-precipitation regions and fewer and weaker events in low-precipitation regions (Trenberth, 2011). This clear dichotomy is shown, with increases of 10–40 % mainly in northern Europe and decreases of up to 20 % in the Mediterranean region and southeastern Europe (DWD, 2019). A similar trend can be seen in Germany, with annual precipitation budgets of more than 800 mm in most regions in west and south Germany, but only 400–500 mm  $y^{-1}$  in the northeast (e.g. areas in Brandenburg and Mecklenburg-Western Pomerania; Schappert, 2018). As crop yields and related crop productivity depend on various factors such as soil properties or water availability, such agricultural used arid regions could face increasing problems.

Brandenburg, a federal state in northeast Germany including some of the driest regions in entire Germany, uses 48.6% or about 1.44 million hectares of its area for agriculture (Amt für Statistik Berlin-Brandenburg, 2020). Brandenburg is located in the continental characterized climate zone and has a water deficit of about 150 mm over the growing season (Wessolek and Asseng 2006). The focus of agriculture in Brandenburg is on grain production, which faces a variety of challenges due to increasingly dry conditions (Amt für Statistik Berlin-Brandenburg, 2020). The Uckermark region is the most fertile region for agriculture in Brandenburg. It is shaped by glaciation with a hilly to flat-wavy ground moraine landscape whose soils are strongly influenced by soil erosion (Nudiargic Luvisol, Calcaric Regosols, Colluvic Regosols) as well as redoximorphic soils (Stagnosols, Gleysols) (MLUK, 2020). The strong soil heterogeneity and ongoing soil erosion, mainly by tillage, has a great influence on the fertility of the cultivated areas (Sommer et al. 2016). In combination with climate crisis, it is proving difficult to develop land use methods that allow reliable arable farming under these changing conditions.

There is a tight link of carbon and water cycling in such precipitation limited systems. In particular, on eroded soils with limited rootability it becomes highly important because water loss by evapotranspiration (ET) and the water use efficiency of a system (WUE) can largely define its productivity (Tallec et al., 2013). To date, methodologically studying the influence of



small scale soil heterogeneity (e.g. soil erosion) and land use (e.g. soil management) on the dynamics of the water balance (especially ET) separately is challenging. However, the effect of both factors can be significantly different with complex interaction (Bakker et al. 2007; Biggelaar et al. 2003), making a separate response analysis an indispensable prerequisite for the development of site-specific land use procedures adapted to the changing climate conditions. ET describes the total amount of water that evaporates from a given area and is thus defined as the sum of evaporation (E), transpiration (Tr), and interception evaporation (Fohrer et al., 2016; Rothfuss et al., 2021). Generally, ET is one of the most important components of the hydrological cycle in terrestrial ecosystems accounting for up to 100 % of ingoing precipitation (Hanson 1991) and is dominated by transpiration in most terrestrial ecosystems with a share of up to 90 %, indicating that terrestrial vegetation is a dominant force in the global water cycle (Jasechko et al. 2013). Due to the expected increased dependency of a systems productivity on sufficient water supply with ongoing climate change, quantifying the ET plays an important role to achieve a process-based understanding the mitigation potential of different crops to drought in the future and to, e.g., establish a more efficient supplemental irrigation.

Methods to quantify evapotranspiration have been developed from disciplines ranging from plant physiology to hydrology and meteorology and range from plot scale to global estimations. To date, each community and method refers to a specific measurement scale, contains its own uncertainties and comparability between methods is rather low (Drexler et al., 2004; Hamel et al., 2015). A particular challenge in current evapotranspiration research apart from standardized approaches is combining high frequency with multi treatment approaches. At the plot scale for example, eddy covariance systems deliver high frequency estimates of evapotranspiration of a homogeneous system (few hundred to millions of square meters) while currently prevailing manual chamber approaches are able to precisely capture multi treatment effects (<1m<sup>2</sup>) on evapotranspiration but lack temporal resolution. In this regard, modern automated chamber systems allowing a combination of high temporal with multi-treatment observation provide the unique opportunity to test advanced statistical gap-filling approaches able to reproduce not only seasonal budgets but day to day and diurnal variability in ET. Previously often limited to eddy covariance approaches, coupling such advanced statistical approaches (e.g. artificial intelligence and neural network approaches) might be an ideal fusion of measurement frequency and the ability to capture treatment effects like small scale soil differences (Falge et al. 2001a; KIŞI and ÇIMEN 2009).

AgroFLUX – a newly developed research platform centered around an automated gantry crane (FluxCrane) mounted chamber system at the “CarboZALF-D” research site – was initially build to capture the effect of soil type and management on CO<sub>2</sub> fluxes with high spatial and temporal resolution (Vaidya et al., 2021). The adaption of the system to measure ET provided us with the opportunity to analyze stand scale ET fluxes including the development of a data analysis tool for measured ET-fluxes, and test different gap-filling strategies. The aim was to establish an approach that would provide reliable predictions of ET fluxes both in terms of gross seasonal budgets as well as representing diurnal trends for automated canopy chamber systems. We tested five different gap-filling approaches including basic statistic and advanced approaches including artificial intelligence and machine learning approaches. During the growth period of winter rye from mid-September 2020 to the end of June 2021 ET and relevant environmental and plant growth parameters were measured to identify the corresponding drivers



100 of crop evapotranspiration and productivity. The gantry crane system covers a field where three different soil types are present,  
which reflect the erosion gradient typical for the hillside of the hummocky ground moraine landscape of NE Germany. This  
enabled to assess the impact of soil type as well as soil management on crop season ET budgets, seasonal development and  
agronomic WUE. In the following we will examine i) soil-type and management effects on budgets as well as spatio-temporal  
variability of ET fluxes over the growing season as well as on  $WUE_{agro}$  and ii) the suitability gap-filling strategies used in this  
105 study as well as potential ways forward to improve these approaches.

## 2 Material and Methods

### 2.1 Study Site and experimental design

The experimental site is located near Dedelow in the NE of Germany within the Uckermark region ( $53^{\circ} 23' N$ ,  $13^{\circ} 47' E$ ; ~50-  
60 m a.s.l). The typical surface is characterized by the last ice ages, when glaciers shaped the land surface to a hummocky  
110 moraine landscape (MLUK 2020). Today, this landscape is characterized by an intensive agriculture, where only 20% of the  
land is not affected by past and present soil erosion due to tillage and water (Sommer et al. 2008; Wilken et al. 2020) resulting  
in a very high spatial variability of soils (Wehrhan and Sommer 2021) and associated growing conditions for crops (Wehrhan  
et al. 2016). The investigations were carried out on the 100 x 16 m FluxCrane experimental field within the AgroFlux site as  
a part of the interdisciplinary research area CarboZALF-D (Fig. 1a). CarboZALF was initially build to capture the effect of  
115 soil type and management on  $CO_2$  fluxes and face the challenge to establish a robust approach to determine carbon budgets of  
erosion deposition processes within the soil-plant-atmosphere system with high spatial and temporal resolution (Sommer et al.  
2016). There is an elevation difference of one meter and all relevant erosion stages are covered (non-eroded Calcic Luvisol  
(LV-cc), strongly eroded Nudiargic Luvisol (LV-ng) and extremely eroded Calcaric Regosol (RG-ca); see Fig. 1b, e; (Sommer  
et al. 2008; Wehrhan et al. 2016; Vaidya et al. 2021)), according to the soil classification of the IUSS working group (WRB  
120 2014). For our study we used 18 plots in total (organic fertilized), 6 per soil type (Fig. 1c). For the 6 plots per soil type, a  
randomized, full-factorial design, each repeated three fold, was adopted for topsoil dilution vs. non-topsoil dilution (topsoil  
modification - first 8 to 9 cm). During the study period from September 2020 to June 2021 (287 days), winter rye of the hybrid  
variety "SU Piano" was grown with a density of 200 plants per  $m^2$  on an area of 0.176 ha. The novel gantry crane automatic  
chamber system (Fig. 1d) was installed over this study site in 2019 (see (Vaidya et al. 2021)); the gas exchange chambers are  
125 lowered on each plot on round iron frames with a diameter of 1.59 m and a basal area of  $1.99 m^2$ .

### 2.2 Cultivation and manipulation

Because the AgroFLUX sensor platform site is located on a conventionally farmed agricultural area intended to represent a  
variety of soils in the region, soil manipulation, tillage, cultivation and fertilization measures were implemented before and  
during the experiment. For soil manipulation, the first 5 cm of topsoils (1.2 t per plot) were removed from 6 selected plots of  
130 the 12 plots per soil type using an excavator on July 14-15, 2020. Then, a soil pit was excavated (20-21 July, 2020) at the



adjacent field to expose the soil horizons (A, B and C) and for application of an equivalent mass to the former prepared plots. Thus, A1 horizon was applied to the prepared plots of the non-eroded Calcic Luvisol (LV-cc), Bt horizon on the strongly eroded Nudiarctic Luvisol (LV-ng) and Ck horizon to the extremely eroded Calcaric Regosol (RG-ca). In order to exchange equal amounts, both the removed and the applied material were weighted. The next day (22 July, 2020) a heavy tine cultivator was used for slow, deep chiseling (25 cm) of all plots in east-west-direction with subsequent mixing of all manipulated plots by hand. Finally, the chamber frames were reinstalled. In the following, the resulting treatments of the same soil types are labelled as "manipulated" (m) and "non-manipulated" (n-m).

The actual tillage prior to sowing took place just before seeding on September 17, 2020. For this, the frames were removed and the soil was loosened to a depth of 25 cm in west-east-direction. Sowing was done with a power harrow-drill combination. Organic fertilization was applied to all plots per soil type, with each 3 plots manipulated and 3 plots non-manipulated, using digestate ( $10 \text{ m}^3 \text{ ha}^{-1}$ ) on September 16, 2020. Due to uneven field emergence, replanting had to be done in all non-manipulated plots within the frames (LV-cc: 13 plants per plot; LV-ng: 40 plants per plot; RG-ca: 82 plants plot). For general plant protection and soil treatment, herbicides were applied to the field during the growing season (e.g. Roundup / glyphosate).

### 2.3 Gantry crane system description and gas exchange measurements

The ET flux measurements were carried out by a novel automated chamber system using a 5-meter-high gantry crane traveling on two 110m tracks which has been described in detail by (Vaidya et al. 2021). Briefly, the Gantry Crane carries two transparent chambers made of polymethyl methacrylate (PMMA; A:  $1.986 \text{ m}^2$ ; V:  $4.621 \text{ m}^3$ ). The system, designed by Pfannenstiel ProProject GmbH (Bad Tölz, Germany), is capable of moving in three dimensions: the x-axis for movement along the track, the y-axis for movement perpendicular to the track, and the z-axis for vertical chamber movement. Since the two chambers do not move independent from each other along the track, frames where arranged in rows, from which each half was measured by one chamber is parallel. To ensure airtight sealing during chamber deployment, steel frames were used and additionally equipped with a foam ring to further increase the chambers bearing surface, while deployed.

### 2.4 Input parameters for gap filling

#### 2.4.1 Environmental Parameters

Relative humidity (RH) [%] was measured simultaneously during the ET flux measurements outside the chambers, while temperature (T) [ $^{\circ}\text{C}$ ] and photosynthetically active radiation (PAR) [ $\mu\text{mol m}^{-2} \text{ s}^{-1}$ ] were measured both, outside as well as inside the chambers. Like precipitation (Pr) [mm], soil moisture (SM; 13 to 18 cm depth) [%] was measured at an adjacent experimental field.



## 2.4.2 Plant specific parameters

160 Spectral plant indices, such as the ratio vegetation index (also simple ratio (SR); RVI) were manually recorded weekly for all  
18 subplots using a near-infrared (NIR)/visible light (VIS) double, 2 canal sensor device (SKR 1850, Skye Instruments Ltd.,  
UK) mounted on a 1.8 m handheld pole (Görres et al. 2014; Kandel et al. 2013), connected to a CR1000 data logger (Campbell  
Scientific Ltd., USA). The double, 2 canal sensor device consist of an up- and downward sensor, measuring the incoming  
(VISi) and reflected (VISr) VIS at a wavelength of  $656 \pm 10$  nm and incoming (NIRi) and reflected (NIRr) NIR at  $780 \pm 10$  nm.  
165 The upward sensor was fitted with a cosine-correction diffusor for measurements of the incident radiation, while the downward  
sensor had a  $25^\circ$  cone field of view, thus covering an area of  $0.5 \text{ m}^2$  during measurements. For each plot, 3 successive 10  
seconds (=10 records) measurements were performed. The RVI was used as an indicator for standing crop biomass and is  
close to zero for a fallow surface and increases as plant cover increases. The RVI was calculated following Equ. 1:

$$170 \quad RVI = \frac{\frac{NIRr}{NIRi}}{\frac{VISr}{VISi}} \quad (1)$$

Since only weekly measurement data were available from plot wise RVI, daily RVI data was obtained by fitting a sigmoidal  
function for initial plant growth in autumn up to a stagnation in winter and polynomial function for shoot elongation and later  
on senescence during spring growth and summer ripening, respectively (Fig. A1). No plant growth was assumed during the  
further called “non-growing season” from November 24, 2020, to March 22, 2021, because average daily temperatures were  
175 mostly below  $5^\circ\text{C}$  (<3 consecutive days).

## 2.5 ET flux calculation and gap filling

The workflow included various steps to pre-process data obtained by the gantry crane automatic chamber system, calculate  
ET fluxes and finally applying and validating the different gap-filling procedures (Fig. A2).

### 2.5.1 ET Flux calculation

180 ET fluxes were determined by measuring the development of chamber headspace  $\text{H}_2\text{O}$  concentrations (4 sec frequency) over  
chamber deployment time of 7 minutes in a flow-through non-steady-state (FT-NSS) mode (Livingston and Hutchinson 1995),  
using two infrared gas analyzers (one per chamber; LI-COR 850, Licor Biosciences, UK). The plots were measured up to 24  
times a day in order to be able to detect daily variations. Diurnal ET fluxes considered in this study were calculated for the  
period from September 17, 2020 (sowing of winter rye), until harvest of winter rye on June 30, 2021. ET flux calculation was  
185 performed based on the ideal gas equation (Eq. 2) modified by (Hamel et al. 2015) using an adapted R-script, based on those  
presented by (Hoffmann et al. 2015).

$$ET_{flux} = \frac{c_{\text{H}_2\text{O}} \times P \times M_{\text{H}_2\text{O}}}{R \times T} \quad (2)$$



With  $ET_{flux}$  [ $mmol\ m^{-2}\ s^{-1}$ ] being the evapotranspiration rate,  $c_{H_2O}$  the moles of water per total moles present,  $P$  the gas pressure  
190 [Pa],  $M_{H_2O}$  the molar mass of water [ $18\ g\ mol^{-1}$ ],  $R$  the gas constant [ $8.314\ m^3\ Pa\ K^{-1}\ mol^{-1}$ ] and  $T$  the temperature [K] inside  
the chamber. To prevent a disturbance due to initial chamber headspace air homogenization, the first 15% of each measurement  
were discarded prior to flux calculation. The temporal change was determined by linear regressions on several subsets of the  
data generated based on a variable moving window with a starting window size of 1:20 minutes (20 consecutive data points)  
and a maximum length of 2 minutes (30 consecutive data points). This procedure resulted in several ET fluxes for each  
195 measurement, from which the best flux was subsequently selected using a set of soft and hard criteria. Soft criteria included:  
(i) checking whether the conditions for the application of a linear regression were fulfilled (normality, variance homogeneity,  
linearity); (ii) no outliers were present ( $\pm 6 \times IQR$ ); (iii) temperature variation during the measurement was  $< 1.5\ ^\circ C$ . Calculated  
fluxes per measurement that did not meet the quality criteria were discarded. Afterwards applied hard-criteria reduced  
potentially remaining multiple fluxes per measurement further to the ideal ET flux. Since the air in the chamber headspace  
200 reached higher water saturation with increasing time, hard criteria were based on the selection of the flux which showed the  
shortest temporal distance to the start of measurement and had the maximum length.

During the measurements, various events could lead to erroneous ET fluxes such as e.g. fog, sensor failures, or chamber  
leakage due to failure in chamber deployment. Erroneous fluxes were hence discarded, such as e.g., in May 2021 (sensor  
failure) or after 23 June 2021. In addition, potential differences of the measurements between the sensors of both chambers  
205 were evaluated by the measurements of ambient air during periods of no chamber deployment.

### 2.5.3 ET flux Gap-filling

To gap fill ET fluxes, five different gap filling approaches were used and compared with each other. Gap-filling procedures  
included: 1.) "Mean diurnal variation" (MDV) as a simple statistical approach; two empirical approaches, namely 2.) "non-  
linear regression" (NLR) and 3.) "Look-Up-Tables" (LUT) as well as, with 4.) "Support Vector machine" (SVM) and 5.)  
210 "artificial neural network with Bayesian regularization"(ANN\_BR) two machine learning approaches.

MDV (Falge et al. 2001b; Moffat et al. 2007) is used to calculate missing hourly values through interpolation of values  
measured at the same hour during adjacent days. Thus, for the season with 286 days, the missing values were calculated for  
every hour, generating 24 values per day.

NLR is based on parameterized non-linear equations using the mean least square method to express the relation between ET  
215 and  $T$ ,  $RH$ ,  $SM$ ,  $PAR$  and  $RVI$ . Half-hourly values were predicted using the predictor variables and obtained function  
parameters.

Gap-filling missing ET fluxes using the LUT approach is based on the assumption of similar ET fluxes during similar  
environmental conditions, whereby similarity is defined through a number of thresholds for the different environmental  
variables. Thus, missing ET-fluxes can be predicted based on the environmental conditions as well as the  $RVI$  associated with  
220 the missing data. To do so, measured ET-fluxes per subplot were split into different classes ( $c_{sturges}$ ) based on  $T$ ,  $RH$ ,  $SM$ ,  $PAR$



and RVI, with their class limits determined by Sturges rule (Equ. 3, (Harkins 2022)). Within this study, on average, 12 classes of equal size were formed covering the range of all parameters.

$$C_{sturges} = \frac{1+3.32 * \log(n)}{\log(10)} \quad (3)$$

225

Gaps in ET-fluxes were subsequently filled with the average ET flux of the class corresponding to obtained environmental parameters within the gap. In case, no class could attributed to measured environmental conditions within a gap, the average ET flux was used.

230 SVM is a black-box-model, where a computer algorithm learns by teaching data to assign values to objects or classes (Noble 2006). As mentioned by (Kim et al. 2020), the SVM uses a slack variable to circumvent unseparated parameters due to noise or extreme values in the data, as well as the radial basis kernel function based on previous SVM studies for upscaling fluxes (e.g. Ichii et al. 2017; Xu et al. 2018).

235 In comparison, ANN\_BR is a combination of a purely empirical nonlinear regression model with a stochastic Bayesian algorithm for regularizing the network training (Schmidt et al. 2018). An artificial neural network (ANN) consists of nodes connected by weights representing the regression parameters (Bishop and others 1995; Hagan et al. 1996; Moffat et al. 2007; Kubat 1999; Rojas 1996). The network is trained by providing it with sets of input data such as the environmental and plant-specific parameters mentioned earlier and the associated output data in the form of e.g. ET flux values. Similar to (Moffat et al. 2007), all techniques evaluated use the classical back-propagation algorithm, where the training of the ANN is performed by propagating the input data through the nodes via the weighted connections and then back-propagating the error and adjusting  
240 the weights so that the network output optimally approximates the ET-fluxes. Subsequent to this training, the underlying dependencies of the ET fluxes on the environmental and plant-specific input variables are mapped to the weights and the ANN is used to predict half-hourly ET fluxes, where the performance of the ANN depends on several criteria.

## 2.6 Seasonal budgets of ET and Water Use Efficiency

245 Seasonal budgets of ET were determined using half-hourly ET values predicted by SVM. Daily averages and seasonal budgets of ET were formed in order to view the development over the entire growth period. The amount of plant biomass in dry mass (DM) [kg] was recorded during harvest treatment wise, which, in combination with  $ET_{sum}$  yields the agricultural water use efficiency  $WUE_{agro}$  ((Hatfield and Dold 2019), Equ. 4). This is the  $WUE_{ABG}$  variant of  $WUE_{agro}$ , as the dry mass is total aboveground biomass (Katerji et al. 2008).

$$250 \quad WUE_{agro} = \frac{DM}{ET_{sum}} \quad (4)$$





## 2.7 Statistical analysis

All calculations were performed using the statistic-software R (R Core Team, 2021) version "4.0.4". Therefore, several packages (Table B1) were used to calculate the ET fluxes and to perform subsequent gap-filling as well to visualization of results. To check the general precision and accuracy of all gap-filling approaches, all measured values were compared with associated predicted values treatment wise. Additionally, k-fold cross validation ( $k = 5$ ) was performed on the resulting ET data to test the predictive outcome of the approaches and ensure robust statistics. Then, all the coefficient of determination ( $r^2$ ), mean absolute error (MAE), normalized root mean square error (NRMSE) and Nash-Sutcliffe efficiency (NSE) were calculated and used to define the most accurate approach for the given setup (Moriassi et al. 2015). To determine the parameters impact on ET, linear and non-linear models were used. Lastly, differences of  $ET_{sum}$ , DM and  $WUE_{agro}$  between treatments were tested with the Kruskal-Wallis-test.

## 3. Results

### 3.1 Environmental parameters

The long-term (1991 to 2020; ZALF) mean annual air temperature in this region is  $8.8^\circ\text{C}$  with a mean annual precipitation and potential evapotranspiration of 467 mm and 637 mm, respectively (ZALF research station, Dedelow). Compared to that, the study period was significantly warmer and wetter with mean temperature of  $9.6^\circ\text{C}$  and an annual precipitation of 508 mm between July 1, 2020 and June 30, 2021. Temperatures (Fig. 2a) were above average in the fall and winter period as well as June, 2021. On the other hand, April and May, which are crucial for crop growth, were colder and also drier. Daily mean relative humidity (rH) ranged between 50 % and 92.4 % with increasing diurnal variation in warm periods. Photosynthetic active radiation (PAR) (Fig. 2b) largely reflected the seasonal variation of the day length with a maximum of  $1860 \mu\text{mol m}^{-2} \text{s}^{-1}$  (half hourly measurements), and reduced values during longer storm events and high cloud cover. The relative soil moisture at 13 to 18 cm depth largely reflects the intensity of precipitation events (Fig. 2c), ranging from 12 % to 29 %. One exception is a prominent increase in mid-February that can be attributed to low temperatures and subsequent snowmelt. The largest precipitation events ( $> 10 \text{ mm d}^{-1}$ ) in the observation period occurred in the observed period on September 26, 2020 with 12 mm, on December 24, 2020 with 15 mm and on February 3, 2021 with 16 mm. With respect to soil moisture, a sharp downward trend and no response to precipitation events is evident from late April onward. However, this can be explained by a high water consumption by the fully developed crop stand and canopy interception. Shallower soil moisture sensors at 3 to 8 cm (not shown) indeed responded to these precipitation events albeit weakly.

### 3.2 Plant development

RVI estimates are based on weekly measurements. Two temporal periods in particular were relevant for plant growth: i) the period from germination to the non-growing season in winter; and ii) the growing period after winter until harvest (Fig. A1).



The maximum RVI values were all reached at a similar time (09. - 13.05.2021). In this regard, the manipulated non-eroded soil of “LV-cc” had the highest RVI (~22.16), while the non-manipulated showed minor values (~17.19). In comparison, the strongly eroded soil of “LV-ng” revealed a reversed pattern with a high RVI for non-manipulated (~18.53) and low RVI manipulated (~13.81) treatments. The extremely eroded soil of “RG-ca”, on the other hand, showed nearly no differences for manipulated and non-manipulated treatments (~12.72, ~12.49). Apart from that, manipulated treatments showed a greater maximum standard deviation than non-manipulated treatments (LV-cc: 5.2 < 6.6; LV-ng: 4.7 < 6.1; RG-ca: 1.6 < 6.2). Clearly higher RVI values were reached in non-eroded and strongly eroded soils compared to extremely eroded soil only during the first growing season in fall of 2020 until the non-growing season. Thus, mean RVI values of ~4.96 to 7.81 were obtained for non-eroded and strongly eroded soils, while the extremely eroded soils had mean RVI values of only ~3.22 (manipulated) and ~3.61 (non-manipulated).

### 3.3 ET Fluxes

A total of 13,011 ET flux measurements were performed, resulting in approximately 2,169 measurements per treatment. ET fluxes differ mainly between soil types (Fig. 3) with minor differences between non-manipulated and manipulated treatments of the same soil type. The seasonal trend of the ET-fluxes is similar for all treatments: a short growth phase after germination is followed by a drop in fluxes until the non-growing season in winter, when hardly any plant activity is found due to low temperatures. At the end of the non-growing season, fluxes in the magnitude of those observed in fall occur quickly and subsequent rapidly increase. On the non-eroded soil (LV-cc) this rapid increase continued into June, while the eroded soils (LV-ng and RZ-ca) showed their peak already in May. Notably, there is a data gap from late April to late May due to sensor failure.

### 3.4 Gap filling and validation

Figure 4 shows the calibration model-performance of the different tested gap-filling approaches as 1:1-agreement plots with associated coefficients of determination ( $r^2$ ). Pronounced differences of tested gap-filling approaches in terms of respective calibration statistics could be found. NLR shows a clear overestimation at low and underestimation of higher ET fluxes. Compared to that, MDV more accurately predicts low/high ET fluxes, but is characterized by a much lower precision due to a higher variance. Among all gap filling approaches, displayed  $r^2$  (> 0.89) and NSE (> 0.9; see table 1) indicate a good prediction for SVM, ANN\_Br and LUT over the entire range of observed ET fluxes. Considering the k-fold-cross validation (Fig. 5, table 2), one can quickly see that LUT is not suitable due to allocation problems while ANN\_Br and SVM also perform well. Statistically, ANN\_BR and SVM were similarly good in predicting observed ET fluxes (table 1 and 2) even if they show a small tendency to overestimate low ET fluxes. However, gap-filled ET fluxes using ANN-BR showed a large number of negative ET fluxes over the entire non-growing season, which is generally less realistic. Hence, we chose SVM to gap-fill ET flux data and predict crop season budgets.



### 3.5 Seasonal ET budgets, temporal dynamics and treatment differences

In order to compare the individual treatments, daily and cumulative ET budgets were calculated (Fig. 6). ET was affected by  
315 T, RH, PAR, and RVI, whereas only a small correlation was found with SM (Fig. 7; table B2). Higher ET fluxes were induced  
by increases in T, PAR and RVI, whereas increasing RH resulted in lower ET fluxes. The seasonal ET budgets ( $ET_{sum}$ , Fig.  
8a) range between  $197.74 \pm 36.36$  mm (LV-cc n-m) and  $169.66 \pm 24.28$  mm (RG-ca m). In general, increasing erosion tends  
to a decrease in  $ET_{sum}$ . Statistical analysis of the correlations revealed that no significant difference was found between  $ET_{sum}$   
of the different treatments. DM and WUE, on the other hand, differed significantly between treatments (Kruskal-Wallis-Test,  
320 DM:  $\chi^2 = 14.58$ ,  $df = 5$ ,  $p = 0.01$ ; WUE:  $\chi^2 = 11.15$ ,  $df = 5$ ,  $p = 0.05$ ).

### 3.6 Crop productivity and WUE

The amount of plant biomass in dry mass (DM) [kg] is decreasing from non-manipulated to manipulated and less eroded soil  
types to more eroded soil types. DM ranges from  $1.5 \pm 0.13$  kg m<sup>-2</sup> for "LV-cc n-m" to  $0.85 \pm 0.2$  kg m<sup>-2</sup> for "RG-ca m".  
WUE<sub>agro</sub> is decreasing from less eroded to more eroded soil types ranging from  $7.73 \pm 1.07$  g DM kg<sup>-1</sup> H<sub>2</sub>O to  $4.98 \pm 0.76$  DM  
325 kg<sup>-1</sup> H<sub>2</sub>O (Fig. 8).

## 4 Discussion

ET is the main ecosystem response variables to drought and mostly measured or modelled on a larger scale by e.g. measurement  
systems such as eddy covariance, Bowen ratio or even satellite remote sensing. These methods are unsuitable for assessing  
small scale differences and do require great experimental care or errors can lead to serious economic losses due to incorrect  
330 water management (Allen et al. 2011; Burba and Verma 2005; Hargreaves 1989). Here, the used, new automated chamber  
system, which is based on a gantry crane combined with complex gap-filling approaches, offers an unprecedented opportunity  
to combine benefits of all methods (high temporal resolution of e.g. eddy covariance with high spatial resolution of chamber  
measurements) with less disadvantages (e.g. atmospheric disturbances due to permanently installed chambers). It measure ET  
reliably in high-resolution, while allowing for the assessment of treatment effects on ET (in this case soil type and  
335 management). We can see, that differences in ET over the growing season as well as between soil types and management  
options result from a variety of factors. In the following we will discuss i) soil-type and management effects on budgets as  
well as spatio-temporal variability of ET fluxes over the growing season as well as on WUE<sub>agro</sub> and ii) the suitability gap-  
filling strategies used in this study as well as potential ways forward to improve these approaches.

### 4.1 Seasonal variability, soil and treatment differences in ET fluxes and WUE

340 Over the entire growing period, ET fluxes responded on the long term particularly to crop growth, first during the establishment  
period in fall (mid of October to mid of November) and then again during the main growth period in spring (end of March to  
mid of May). The close relation of measured ET flux dynamics to obtained RVI (Fig. 7) (e.g. Hanks et al. 1969), can be



associated with increasing transpiration rates that superimpose the suppressive effects of increasing canopy biomass (e.g. increases in LAI or RVI) on soil evaporation (Dubbert et al. 2014; Groh et al. 2020). More dynamically, ET reacted to changes  
345 in environmental conditions, particularly temperature and relative humidity which together define the vapour-pressure deficit (VPD) as well as PAR. In particular, crops that have been bred to prioritize carbon gain over water conservation will tend to respond to rising VPD strongly (Dubbert et al. 2014; Massmann et al. 2019). In summary, air temperature, humidity and PAR together with increasing biomass (expressed as higher RVI) control ET variability during the peak growth period in spring until harvest. Soil moisture, on the other hand, did not have a limiting effect on ET during the period considered. This is  
350 noteworthy since the Uckermark region has an  $ET_{pot}/Pr$  ratio of nearly 1 which is regarded as a threshold value between systems that are energy ( $<1$ ) vs. water limited ( $>1$ ; DWD 2022).

The soil types in the region vary in their suitability for agricultural cultivation (MLUK 2020). Luvisols show a good water budget due to their clay-depleted deep topsoils in combination with the clay-enriched and mostly decalcified subsoils and thus belong to the most fertile soils in Brandenburg (MLUK 2020; Stahr 2022). Regosols are generally only moderately suitable  
355 for arable farming but cultivated in the studied region. They are usually found on hilltops and are characterized by C horizons near to the surface, lack of depth development, and limited rootability due to the dense, high carbonate parent material, resulting in a low water availability and plant growth (Herbrich et al. 2018). It is a typical soil type, formed by erosion of agricultural Luvisols. As a result of these conditions and the associated increase in drought and heat events in Central Europe (Spinoni et al., 2018), regional farmers might become limited in their choice of crops grown due to water availability. Here, our results  
360 indicate significant differences between measured soil types in DM and  $WUE_{agro}$  but no significant differences between  $ET_{sum}$ , although we see a clear decreasing trend along the erosion gradient and topsoil manipulation of the three studied soil types ( $198 \pm 36$  mm to  $170 \pm 25$  mm). This was expected due to the supposed lower rootability and soil fertility, but the difference was likely reduced by the comparatively wet year of observation. A dry spell during the main growth period could lead to larger differences here. Since there are no significant differences in  $ET_{sum}$ , it can be concluded that the observed  
365 agroecosystems was mostly energy limited, however it is very likely that the  $ET_{pot}/Pr$  ratio will vary considerably between wetter and drier years and between different crops (particularly winter vs. summer crops). Winter crops and especially winter rye, are more resilient to drought (Ehlers 1997) and an investigation with other crops and management strategies could lead to a higher decrease in ET with soil erosion. The difference in DM for the observed year was much larger compared to the ET differences in turn driving soil type or erosion effects on the water use efficiency ( $WUE_{agro}$ ). In a period of consecutive dry  
370 years e.g., a lower WUE could additionally have a negative effect on the water and carbon balance of the whole system, since the water consumption becomes largely unproductive (up to 36% less yield per used amount of water; Meena et al. 2020). This could further exacerbate the drought.

One of our expectations was that differences in ET crop season budgets would result mainly from differences during the main vegetation period from April to harvest due to variations in biomass and thus transpiration. In contrast, differences in ET  
375 budgets between soil types, rather occur continuously throughout the period with very little variation. It is noticeable that ET-fluxes of eroded treatments prior the growing season are lower than those of non-eroded plots for long periods. Although the



growing season between April and June is responsible for a large portion of total evapotranspiration for the entire period, ranging from ~ 64% to ~ 70%, it is only responsible for a small portion of differences, with a maximum of ~ 12.3 mm from the non-eroded plot. The prior period, on the other hand, is responsible for a difference of up to ~ 15.8 mm from non-eroded plots, although it accounts for only ~ 30 % to 36 % of total evapotranspiration. However, it should be noted that mean differences per day of about 0.14 mm in the growing season was about 75% higher than in the previous period with about 0.08 mm per day. This is interesting, because it suggests that the reason behind the soil type differences in ET are caused by static differences (e.g. lower biomass) rather than dynamic differences (e.g. the vegetation responses to environmental drivers or drought). Here, partitioning ET into evaporation and transpiration (e.g. Rothfuss et al. 2021) could help explain the reasons for small-scale ET variability.

Beside this static differences, high ET fluxes could be detected at the beginning of the growing season which could be explained by a lower soil cover. This may be related to the fact that vegetation cover due to uneven field emergence, which is visible in the RVI, can largely reduce soil evaporation (Dubbert et al. 2014; Hu et al. 2009; Raz-Yaseef et al. 2012; Wang et al. 2012). However, the vegetation period studied can be described as rather wet compared to long-term environmental conditions and it will be interesting to monitor this for a number of years differing in environmental and hydrological conditions as well as for different crops. For example, the more eroded soil types are reported to lead to decreases in rooting depths (Öttl et al. 2021; Sommer et al. 2016; Herbrich et al. 2018). In dry years, this may very well lead to a more pronounced response in ET flux dynamics between the treatments particularly in the spring summer transition compared to results from the present study, when the crop benefits stronger from deep water sources during pronounced dry spells (Thorup-Kristensen et al. 2020). Finally, results for evapotranspiration from nearby lysimeters suggested annual gross ET budgets of around 300 mm to 600 mm in years between 2014 and 2018 with varying crops (Groh et al. 2020). The budgets estimated in (Groh et al. 2020), however, were spanning over the entire year, whereas in this study budgets were calculated to the crop period (only ~9 months and the summer months with high  $ET_{pot}$  excluded), explaining the overall higher budgets. In addition, temperatures and precipitation were below average in April and May during the growing season under consideration which result in lower ET thus matching our results. Thus, our ET budgets seem sensible overall, however, a direct comparison between the new gantry crane chamber system, lysimeters and potentially drone based observations of ET would be advisable particularly in light of ongoing discussions surrounding method constrains of estimating ET across scales (Ding et al. 2021; Ghiat et al. 2021; Hamel et al. 2015).

#### 4.2 Gap-filling approaches

The experimental design of the used gantry crane system with a high amount of different treatments and measurements of diurnal cycles coupled with unsuitable climate conditions causes data gaps that need to be filled. The challenge was composed of two main elements: i) the correct quantification of  $ET_{sum}$  and ii) a realistic prediction of diurnal variations both during winter (low ET) and summer (high ET). With respect to the gap-filling approaches compared, it was determined that all approaches provided fairly plausible results for accounting of  $ET_{sum}$ . While LUT showed good calibration results, allocation problems



410 caused the least predictive ability during validation over the entire range of measured ET fluxes. While some studies received  
also fairly plausible results for LUT and MDV (Boudhina et al. 2018; Falge et al. 2001a; Moffat et al. 2007), adjusting the  
classes of the LUT could further improve the results of this approach. However, due to the significantly good results of the  
other approaches, this was not done yet. Additionally, other studies found out that MDV (as well as LUT) especially performs  
worse with increasing large gaps (Moffat et al. 2007; Kim et al. 2020). Especially for conditions, where no measurements  
415 could take place due to environmental conditions, the fact that MDV takes averaged values of close measurements with good  
measurement conditions could explain the bad predictions. Same for LUT, since no classes could be created for conditions no  
measurements took place. The machine learning approaches SVM and ANN\_BR, on the other hand, also performs well here.  
For seasonal variability and budgets we also achieved the best performance with approaches ANN\_BR and SVM. However,  
the best approach for gap filling can vary depending on the application and investigated parameter. For example, in gap-filling  
420 methane fluxes using eddy covariance (Kim et al. 2020), ANN\_BR was superior to SVM. Additionally, results of other studies  
like (Shrestha and Shukla 2015), who tried to predict actual evapotranspiration ( $ET_a$ ) measured with lysimeters with different  
approaches (e.g. ANN\_BR and SVM) and crops (pepper, watermelon) in a sub-tropical environment resulting in best  
predictions with SVM (pepper: 204.7 mm lysimeter vs. 181.8 mm SVM; watermelon: 231.71 mm lysimeter vs. 189.83 mm  
SVM) found a overestimation of low- and underestimation of high-fluxes of ANN\_BR and SVM. We were able to detect this  
425 tendency only with a slight overestimation of small fluxes. In comparison to empirical calculations, another study by (KIŞI  
and ÇIMEN 2009) worked out, that SVM performed even better for  $ET_0$  predictions (FAO-56 PM) with solar radiation,  
temperature, relative humidity and wind speed compared to commonly used empirical approaches like CIMIS-Penman,  
Hargreaves, Ritchie or Turc and similar with reduced parameters (solar radiation and temperature). Thus, using other  
environmental parameters such as wind speed could also improve SVM results for our application. Additionally, it must be  
430 noted that the quality of SVM (and ANN\_BR) predictions is highly dependent on the amount of data (Chia et al. 2020; Abudu  
et al. 2010).

### 4.3 Conclusion and outlook

Filling data gaps using statistical and empirical approaches is used in many fields like calculations of reference ET ( $ET_0$ ) with  
limited meteorological parameters (Chia et al. 2020) or actual ET ( $ET_a$ ) from eddy-covariance measurements as well as plant  
435 chamber measurements (Hui et al. 2004; Moffat et al. 2007; Falge et al. 2001a; Falge et al. 2001b; Hamel et al. 2015; Kübert  
et al. 2019). The connection between gap-filling approaches in combination with the described continuous high-resolution  
long-term ET measurements of numerous small-scale treatments gives additional opportunities to observe the progression of  
ET over an entire growing season. In comparison to eddy covariance measurements (e. g. Boudhina et al. 2018; Simpson et al.  
2019), this approach is able to point out small scale treatment differences like soil type differences and associated erosion  
440 stages at a heterogeneous field with a relatively high number of different treatments simultaneously. Additionally, there is not  
such a big impact through the system compared to e.g. permanently installed plant chambers or manually conducted approaches  
which deal with condensation problems due to fix installed tubing and inappropriate air mixing inside the chamber (e. g.



(Hamel et al. 2015). This problem does not exist with the automated gantry crane system, since there are permanent measurements and a consistent air flow through the system.

445 The study could demonstrate, that the gantry crane system used provided plausible ET fluxes. While it has many benefits over other measurement systems, there are some particular challenges. For example, the crane and the installed measuring equipment have to be checked regularly and in case of strong winds a manual shutdown and fixation have to be performed. With respect to the ET measurements, there might also be an underestimation of the automated chambers, which has already been found in comparison to the measurement with the eddy covariance in other studies (e.g. Simpson et al., 2019). To shed

450 light on this problem, a more detailed comparison could be made in the future with nearby lysimeters with the same soil types. In order to the gap filling approaches, only the support vector machine (SVM), artificial neural network with Bayesian regularization (ANN\_BR) and non-linear regression (NLR) approaches are suitable for a consistently consideration of diurnal variations at this stage, while all approaches provided plausible data for the seasonal period. Thereby, gap filling is highly dependent on data quality, with larger gaps leading to greater problems. Since the gantry crane was unable to provide data for

455 extended periods (up to approx. 1. month), this led to uncertainties. However, the studied measurement period was the first full crop period observed by the novel infrastructure and these initial problems will be very likely mitigated in the future through reliable and regular maintenance. One gap in particular should be highlighted in the data considered: hardly any data could be collected with chamber 1 for an extended period of time due to a sensor problem in May (May 1 to May 29.). Although the gap could be filled reasonably well with the SVM, with validation statistics indicating a reasonable predicting performance

460 (Table 2), an underestimation is possible due to the large gaps importance of this month for plant growth. Additionally, an interruption of the non-growing season could cause better results, since it can be assumed that already in short warmer period's plant activity is to be found (<3 days less than 5°C). Here, e.g. several non-growing seasons could represent the plant growth much better and lead to a further increase of the predicted accuracy.

Despite these small flaws, the system has a very large potential to bring new insights into water-flux dynamics and budgets

465 and, in combination with measurements of NEE into growths season dynamics of water use efficiencies in the future. On the one hand, the different effects of soil types and related erosion levels on other crops could be investigated, and on the other hand, related knowledge for cultivation could be gained. Furthermore, in contrast to other established approaches to quantify ET at the plots scale, the novel system is unique in its potential to combine it with innovative measurements such as stable water isotopes (Dubbert et al. 2014; Kübert et al. 2020). Stable water isotopes could be used to separate the evapotranspiration

470 into transpiration and evaporation, [which is of crucial importance for the terrestrial water balance and for the prediction of future ecosystem feedbacks] (Groh et al. 2020). This could lead to further plant specific knowledge like e.g. root water uptake and uptake depths of different crops. Especially the possibility of automated high-resolution long-term measurements of these parameters is unique and could provide further knowledge about the ratio of evaporation and transpiration in the course of the season, since we expect huge changes through drought here.



## 475 **5 Code availability**

The codes produced for this study are available from the corresponding author upon request.

## **6 Data availability**

The data sets produced for this study are available from the corresponding author upon request.

## **7 Author contributions**

480 AD, MD conceived and planned the study. MS, GV, MH supervised automated measurements and conducted complimentary field measurements. AD analyzed the data and wrote a first version of the manuscript. All authors contributed to manuscript writing.

## **8 Competing interests**

The authors declare that they have no conflict of interest.

## 485 **9 Acknowledgements**

The authors acknowledge funding by the German Federal Ministry of Food and Agriculture (FNR Grant: 22404117) and the German Science Foundation (DFG Grant DU1688/6-1). The authors are very grateful to the Pfannenstiel ProProject GmbH for the excellent collaboration in designing as well as constructing the gantry crane system and ATTEC Automation GmbH for programming the system control. The study was a part of the CarboZALF project of the Leibniz Centre for Agricultural  
490 Landscape Research (ZALF). The CarboZALF project was financially supported by the German Federal Ministry of Food, Agriculture and Consumer Protection (BMELV) and the Ministry of Environment, Health and Consumer (MLUV) of the State of Brandenburg. The authors the Research Station Dedelow of the ZALF for assistance with field measurements.

495





500

### Publication bibliography

- Abudu, Shalamu; Bawazir, A. Salim; King, J. Phillip (2010): Infilling Missing Daily Evapotranspiration Data Using Neural Networks. In *J. Irrig. Drain Eng.* 136 (5), pp. 317–325. DOI: 10.1061/(ASCE)IR.1943-4774.0000197.
- 505 Allen, Richard G.; Pereira, Luis S.; Howell, Terry A.; Jensen, Marvin E. (2011): Evapotranspiration information reporting: I. Factors governing measurement accuracy. In *Agricultural Water Management* 98 (6), pp. 899–920. DOI: 10.1016/J.AGWAT.2010.12.015.
- Amt für Statistik Berlin-Brandenburg (2020): Ernteberichterstattung über Feldfrüchte und Grünland im Land Brandenburg 2019. Available online at <https://www.statistik-berlin-brandenburg.de/>, checked on 8/18/2022.
- 510 Bakker, Martha M.; Govers, Gerard; Jones, Robert A.; Rounsevell, Mark D. A. (2007): The Effect of Soil Erosion on Europe’s Crop Yields. In *Ecosystems* 10 (7), pp. 1209–1219. DOI: 10.1007/s10021-007-9090-3.
- Biggelaar, Christoffel den; Lal, Rattan; Wiebe, Keith; Breneman, Vince (2003): The Global Impact Of Soil Erosion On Productivity: I: Absolute and Relative Erosion-induced Yield Losses. In *Advances in Agronomy* 81, pp. 1–48.
- Bishop, Christopher M.; others (1995): Neural networks for pattern recognition: Oxford university press.
- 515 Blum, Winfried E.H. (2013): Soil and Land Resources for Agricultural Production: General Trends and Future Scenarios-A Worldwide Perspective. In *International Soil and Water Conservation Research* 1 (3), pp. 1–14. DOI: 10.1016/S2095-6339(15)30026-5.
- Boudhina, Nissaf; Zitouna-Chebbi, Rim; Mekki, Insaf; Jacob, Frédéric; Ben Mechlia, Nétij; Masmoudi, Moncef; Prévot, Laurent (2018): Evaluating four gap-filling methods for eddy covariance measurements of evapotranspiration over hilly crop  
520 fields. In *Geosci. Instrum. Method. Data Syst.* 7 (2), pp. 151–167. DOI: 10.5194/gi-7-151-2018.
- Burba, George G.; Verma, Shashi B. (2005): Seasonal and interannual variability in evapotranspiration of native tallgrass prairie and cultivated wheat ecosystems. In *Agricultural and Forest Meteorology* 135 (1-4), pp. 190–201. DOI: 10.1016/J.AGRFORMET.2005.11.017.
- Chia, Min Yan; Huang, Yuk Feng; Koo, Chai Hoon (2020): Support vector machine enhanced empirical reference  
525 evapotranspiration estimation with limited meteorological parameters. In *Computers and Electronics in Agriculture* 175, p. 105577. DOI: 10.1016/j.compag.2020.105577.



- Ding, Jie; Li, Sien; Wang, Hongshuo; Wang, Chunyu; Zhang, Yunxuan; Yang, Danni (2021): Estimation of Evapotranspiration and Crop Coefficient of Chinese Cabbage Using Eddy Covariance in Northwest China. In *Water* 13 (19), p. 2781. DOI: 10.3390/w13192781.
- 530 Drexler, Judy Z.; Snyder, Richard L.; Spano, Donatella; Paw U, Kyaw Tha (2004): A review of models and micrometeorological methods used to estimate wetland evapotranspiration. In *Hydrol. Process.* 18 (11), pp. 2071–2101. DOI: 10.1002/hyp.1462.
- Dubbert, Maren; Piayda, Arndt; Cuntz, Matthias; Correia, Alexandra C.; Costa e Silva, Filipe; Pereira, Joao S.; Werner, Christiane (2014): Stable oxygen isotope and flux partitioning demonstrates understory of an oak savanna contributes up to  
535 half of ecosystem carbon and water exchange. In *Frontiers in plant science* 5, p. 530. DOI: 10.3389/fpls.2014.00530.
- DWD (2019): Klimareport Brandenburg. 1. Auflage. Edited by Deutscher Wetterdienst. Offenbach am Main, Germany.
- DWD (2022): Klimakarten Deutschland. Edited by Deutscher Wetterdienst. Available online at <https://www.dwd.de/DE/leistungen/klimakartendeutschland/klimakartendeutschland.html>, checked on 9/8/2022.
- Ehlers, W. (1997): Zum Transpirationskoeffizienten von Kulturpflanzen unter Feldbedingungen. In  
540 *Pflanzenbauwissenschaften* 1 (3), pp. 97–108.
- Falge, Eva; Baldocchi, Dennis; Olson, Richard; Anthoni, Peter; Aubinet, Marc; Bernhofer, Christian et al. (2001a): Gap filling strategies for defensible annual sums of net ecosystem exchange. In *Agricultural and Forest Meteorology* 107 (1), pp. 43–69. DOI: 10.1016/S0168-1923(00)00225-2.
- Falge, Eva; Baldocchi, Dennis; Olson, Richard; Anthoni, Peter; Aubinet, Marc; Bernhofer, Christian et al. (2001b): Gap  
545 filling strategies for long term energy flux data sets. In *Agricultural and Forest Meteorology* 107 (1), pp. 71–77. DOI: 10.1016/S0168-1923(00)00235-5.
- Fohrer, Nicola; Bormann, Helge; Miegel, Konrad; Casper, Markus; Schumann, Andreas; Bronstert, Axel; Weiler, Markus (2016): Hydrologie. 1. Auflage. Stuttgart: UTB GmbH; Haupt (Utb Basics, 4513).
- Ghiat, Ikhlas; Mackey, Hamish R.; Al-Ansari, Tareq (2021): A Review of Evapotranspiration Measurement Models,  
550 Techniques and Methods for Open and Closed Agricultural Field Applications. In *Water* 13 (18), p. 2523. DOI: 10.3390/w13182523.
- Görres, C.-M.; Kutzbach, L.; Elsgaard, L. (2014): Comparative modeling of annual CO<sub>2</sub> flux of temperate peat soils under permanent grassland management. In *Agriculture, Ecosystems & Environment* 186, pp. 64–76. DOI: 10.1016/j.agee.2014.01.014.



- 555 Groh, Jannis; Diamantopoulos, Efstathios; Duan, Xiaohong; Ewert, Frank; Herbst, Michael; Holbak, Maja et al. (2020): Crop growth and soil water fluxes at erosion-affected arable sites: Using weighing lysimeter data for model intercomparison. In *Vadose zone j.* 19 (1). DOI: 10.1002/vzj2.20058.
- Hagan, M. T.; Demuth, H. B.; Beale, M.; Jesus, O. de (1996): Neural Network Design, Boston. In *PWS Pub. Co. USA*.
- Hamel, Perrine; Mchugh, Ian; Coutts, Andrew; Daly, Edoardo; Beringer, Jason; Fletcher, Tim D. (2015): Automated  
560 Chamber System to Measure Field Evapotranspiration Rates. In *J. Hydrol. Eng.* 20 (2), Article 04014037, p. 4014037. DOI: 10.1061/(ASCE)HE.1943-5584.0001006.
- Hanks, R. J.; Gardner, H. R.; Florian, R. L. (1969): Plant Growth-Evapotranspiration Relations for Several Crops in the Central Great Plains 1. In *Agronomy Journal* 61 (1), pp. 30–34. DOI: 10.2134/agronj1969.00021962006100010010x.
- Hanson, Ronald L. (1991): Evapotranspiration and droughts. In *National Water Summary 1988-89: Hydrologic Events and*  
565 *Floods and Droughts (US Geological Survey Water-Supply Paper 2375)*, pp. 99–104.
- Hargreaves, George H. (1989): Accuracy of Estimated Reference Crop Evapotranspiration. In *J. Irrig. Drain Eng.* 115 (6), pp. 1000–1007. DOI: 10.1061/(ASCE)0733-9437(1989)115:6(1000).
- Harkins, Ray (2022): Sturge’s Rule: A Method for Selecting the Number of Bins in a Histogram, checked on 8/19/2022.
- Hatfield, Jerry L.; Dold, Christian (2019): Water-Use Efficiency: Advances and Challenges in a Changing Climate. In  
570 *Frontiers in plant science* 10, p. 103. DOI: 10.3389/fpls.2019.00103.
- Herbrich, Marcus; Gerke, Horst H.; Sommer, Michael (2018): Root development of winter wheat in erosion-affected soils depending on the position in a hummocky ground moraine soil landscape. In *J. Plant Nutr. Soil Sci.* 181 (2), pp. 147–157. DOI: 10.1002/jpln.201600536.
- Hoffmann, Mathias; Jurisch, Nicole; Albiac Borraz, Elisa; Hagemann, Ulrike; Drösler, Matthias; Sommer, Michael;  
575 Augustin, Jürgen (2015): Automated modeling of ecosystem CO<sub>2</sub> fluxes based on periodic closed chamber measurements: A standardized conceptual and practical approach. In *Agricultural and Forest Meteorology* 200, pp. 30–45. DOI: 10.1016/J.AGRFORMET.2014.09.005.
- Hu, Zhongmin; Yu, Guirui; Zhou, Yanlian; Sun, Xiaomin; Li, Yingnian; Shi, Peili et al. (2009): Partitioning of evapotranspiration and its controls in four grassland ecosystems: Application of a two-source model. In *Agricultural and*  
580 *Forest Meteorology* 149 (9), pp. 1410–1420. DOI: 10.1016/J.AGRFORMET.2009.03.014.
- Hui, Dafeng; Wan, Shiqiang; Su, Bo; Katul, Gabriel; Monson, Russell; Luo, Yiqi (2004): Gap-filling missing data in eddy covariance measurements using multiple imputation (MI) for annual estimations. In *Agricultural and Forest Meteorology* 121 (1-2), pp. 93–111. DOI: 10.1016/S0168-1923(03)00158-8.



- 585 Ichii, Kazuhito; Ueyama, Masahito; Kondo, Masayuki; Saigusa, Nobuko; Kim, Joon; Alberto, Ma. Carmelita et al. (2017):  
New data-driven estimation of terrestrial CO<sub>2</sub> fluxes in Asia using a standardized database of eddy covariance  
measurements, remote sensing data, and support vector regression. In *JGR Biogeosciences* 122 (4), pp. 767–795. DOI:  
10.1002/2016JG003640.
- Jasechko, Scott; Sharp, Zachary D.; Gibson, John J.; Birks, S. Jean; Yi, Yi; Fawcett, Peter J. (2013): Terrestrial water fluxes  
dominated by transpiration. In *Nature* 496 (7445), pp. 347–350. DOI: 10.1038/nature11983.
- 590 Jie, Chen; Jing-zhang, Chen; Man-zhi, Tan; Zi-tong, Gong (2002): Soil degradation: a global problem endangering  
sustainable development. In *J. Geogr. Sci* 12 (2), pp. 243–252. DOI: 10.1007/BF02837480.
- Kandel, Tanka P.; Elsgaard, Lars; Laerke, Poul E. (2013): Measurement and modelling of CO<sub>2</sub> flux from a drained fen  
peatland cultivated with reed canary grass and spring barley. In *GCB Bioenergy* 5 (5), pp. 548–561. DOI:  
10.1111/gcbb.12020.
- 595 Katerji, Nader; Mastrorilli, Marcello; Rana, Gianfranco (2008): Water use efficiency of crops cultivated in the  
Mediterranean region: Review and analysis. In *European Journal of Agronomy* 28 (4), pp. 493–507. DOI:  
10.1016/j.eja.2007.12.003.
- Kim, Yeonuk; Johnson, Mark S.; Knox, Sara H.; Black, T. Andrew; Dalmagro, Higo J.; Kang, Minseok et al. (2020): Gap-  
filling approaches for eddy covariance methane fluxes: A comparison of three machine learning algorithms and a traditional  
600 method with principal component analysis. In *Global change biology* 26 (3), pp. 1499–1518. DOI: 10.1111/GCB.14845.
- KIŞI, OZGUR; ÇIMEN, MESUT (2009): Evapotranspiration modelling using support vector machines / Modélisation de  
l'évapotranspiration à l'aide de 'support vector machines'. In *Hydrological Sciences Journal* 54 (5), pp. 918–928. DOI:  
10.1623/hysj.54.5.918.
- Kubat, Miroslav (1999): Neural networks: a comprehensive foundation by Simon Haykin, Macmillan, 1994, ISBN 0-02-  
605 352781-7. In *The Knowledge Engineering Review* 13 (4), pp. 409–412. DOI: 10.1017/S0269888998214044.
- Kübert, Angelika; Götz, Miriam; Kuester, Emma; Piayda, Arndt; Werner, Christiane; Rothfuss, Youri; Dubbert, Maren  
(2019): Nitrogen Loading Enhances Stress Impact of Drought on a Semi-natural Temperate Grassland. In *Frontiers in plant  
science* 10, p. 1051. DOI: 10.3389/fpls.2019.01051.
- Kübert, Angelika; Paulus, Sinikka; Dahlmann, Adrian; Werner, Christiane; Rothfuss, Youri; Orłowski, Natalie; Dubbert,  
610 Maren (2020): Water Stable Isotopes in Ecohydrological Field Research: Comparison Between In Situ and Destructive  
Monitoring Methods to Determine Soil Water Isotopic Signatures. In *Frontiers in plant science* 11, p. 387. DOI:  
10.3389/fpls.2020.00387.



- Livingston, G. P.; Hutchinson, G. L. (1995): Enclosure-based measurement of trace gas exchange: applications and sources of error. In *Biogenic trace gases: measuring emissions from soil and water* 51, pp. 14–51.
- 615 Louwagie, G.; Gay, S. H.; Sammeth, F.; Ratering, T. (2011): The potential of European Union policies to address soil degradation in agriculture. In *Land Degrad. Dev.* 22 (1), pp. 5–17. DOI: 10.1002/ldr.1028.
- Massmann, Adam; Gentine, Pierre; Lin, Changjie (2019): When Does Vapor Pressure Deficit Drive or Reduce Evapotranspiration? In *Journal of advances in modeling earth systems* 11 (10), pp. 3305–3320. DOI: 10.1029/2019MS001790.
- 620 Meena, Ram Swaroop; Kumar, Sandeep; Yadav, Gulab Singh (2020): Soil Carbon Sequestration in Crop Production. In Ram Swaroop Meena (Ed.): *Nutrient Dynamics for Sustainable Crop Production*. Singapore: Springer Singapore, pp. 1–39.
- MLUK (2020): *Steckbriefe Brandenburger Böden. Sammelmappe*. Edited by Ministerium für Ländliche Entwicklung.
- Moffat, Antje M.; Papale, Dario; Reichstein, Markus; Hollinger, David Y.; Richardson, Andrew D.; Barr, Alan G. et al. (2007): Comprehensive comparison of gap-filling techniques for eddy covariance net carbon fluxes. In *Agricultural and Forest Meteorology* 147 (3-4), pp. 209–232. DOI: 10.1016/j.agrformet.2007.08.011.
- 625 Moriasi, Daniel N.; Gitau, Margaret W.; Prasad Daggupati, Naresh Pai (2015): Hydrologic and Water Quality Models: Performance Measures and Evaluation Criteria. In *Trans. ASABE* 58 (6), pp. 1763–1785. DOI: 10.13031/TRANS.58.10715.
- Noble, William S. (2006): What is a support vector machine? In *Nature biotechnology* 24 (12), pp. 1565–1567. DOI: 10.1038/nbt1206-1565.
- 630 Öttl, Lena Katharina; Wilken, Florian; Auerswald, Karl; Sommer, Michael; Wehrhan, Marc; Fiener, Peter (2021): Tillage erosion as an important driver of in-field biomass patterns in an intensively used hummocky landscape. In *Land Degradation & Development* 32 (10), pp. 3077–3091. DOI: 10.1002/LDR.3968.
- Raz-Yaseef, Naama; Yakir, Dan; Schiller, Gabriel; Cohen, Shabtai (2012): Dynamics of evapotranspiration partitioning in a semi-arid forest as affected by temporal rainfall patterns. In *Agricultural and Forest Meteorology* 157, pp. 77–85. DOI: 10.1016/J.AGRFORMET.2012.01.015.
- 635 Rojas, Raúl (Ed.) (1996): *Neural Networks*. Berlin, Heidelberg: Springer Berlin Heidelberg.
- Rothfuss, Youri; Quade, Maria; Brüggemann, Nicolas; Graf, Alexander; Vereecken, Harry; Dubbert, Maren (2021): Reviews and syntheses: Gaining insights into evapotranspiration partitioning with novel isotopic monitoring methods. In *Biogeosciences* 18 (12), pp. 3701–3732. DOI: 10.5194/bg-18-3701-2021.
- 640 Schappert, Sebastian (2018): Wie wird Niederschlag beim DWD gemessen und wo fällt am meisten? Deutscher Wetterdienst. Offenbach am Main, Germany. Available online at [https://www.dwd.de/DE/wetter/thema\\_des\\_tages/2018/11/28.html](https://www.dwd.de/DE/wetter/thema_des_tages/2018/11/28.html), checked on 8/18/2022.



- Schmidt, Andres; Creason, Whitney; Law, Beverly E. (2018): Estimating regional effects of climate change and altered land use on biosphere carbon fluxes using distributed time delay neural networks with Bayesian regularized learning. In *Neural networks : the official journal of the International Neural Network Society* 108, pp. 97–113. DOI: 10.1016/j.neunet.2018.08.004.
- Shrestha, N. K.; Shukla, S. (2015): Support vector machine based modeling of evapotranspiration using hydro-climatic variables in a sub-tropical environment. In *Agricultural and Forest Meteorology* 200, pp. 172–184. DOI: 10.1016/j.agrformet.2014.09.025.
- Shukla, P. R.; Skeg, J.; Calvo Buendia, E.; Masson-Delmotte, V.; Pörtner, H.-O.; Roberts, D. C. et al. (2019): Climate Change and Land: An IPCC Special Report on Climate Change, Desertification, Land Degradation, Sustainable Land Management, Food Security, and Greenhouse Gas Fluxes in Terrestrial Ecosystems.
- Simpson, Gillian; Runkle, Benjamin R.K.; Eckhardt, Tim; Kutzbach, Lars (2019): Evaluating closed chamber evapotranspiration estimates against eddy covariance measurements in an arctic wetland. In *Journal of Hydrology* 578, p. 124030. DOI: 10.1016/j.jhydrol.2019.124030.
- Sommer, M.; Augustin, J.; Kleber, M. (2016): Feedbacks of soil erosion on SOC patterns and carbon dynamics in agricultural landscapes—The CarboZALF experiment. In *Soil & Tillage Research* 156 (156), pp. 182–184. DOI: 10.1016/j.still.2015.09.015.
- Sommer, M.; Gerke, H. H.; Deumlich, D. (2008): Modelling soil landscape genesis — A “time split” approach for hummocky agricultural landscapes. In *Geoderma* 145 (3-4), pp. 480–493. DOI: 10.1016/j.geoderma.2008.01.012.
- Stahr, Alexander (2022): Bodentypen. Available online at <http://www.ahabc.de/bodentypen/>, checked on 8/19/2022.
- Talleg, Tiphaine; Béziat, Pierre; Jarosz, Nathalie; Rivalland, Vincent; Ceschia, Eric (2013): Crops’ water use efficiencies in temperate climate: Comparison of stand, ecosystem and agronomical approaches. In *Agricultural and Forest Meteorology* 168, pp. 69–81. DOI: 10.1016/j.agrformet.2012.07.008.
- Thorup-Kristensen, Kristian; Halberg, Niels; Nicolaisen, Mette; Olesen, Jørgen Eivind; Crews, Timothy E.; Hinsinger, Philippe et al. (2020): Digging Deeper for Agricultural Resources, the Value of Deep Rooting. In *Trends in plant science* 25 (4), pp. 406–417. DOI: 10.1016/J.TPLANTS.2019.12.007.
- Trenberth, K. E. (2011): Changes in precipitation with climate change. In *Clim. Res.* 47 (1), pp. 123–138. DOI: 10.3354/cr00953.
- Vaidya, Shrijana; Schmidt, Marten; Rakowski, Peter; Bonk, Norbert; Verch, Gernot; Augustin, Jürgen et al. (2021): A novel robotic chamber system allowing to accurately and precisely determining spatio-temporal CO<sub>2</sub> flux dynamics of heterogeneous croplands. In *Agricultural and Forest Meteorology* 296, p. 108206. DOI: 10.1016/j.agrformet.2020.108206.



- 675 Wang, L.; D'Odorico, P.; Evans, J. P.; Eldridge, D. J.; McCabe, M. F.; Caylor, K. K.; King, E. G. (2012): Dryland  
ecohydrology and climate change: critical issues and technical advances. In *Hydrol. Earth Syst. Sci.* 16 (8), pp. 2585–2603.  
DOI: 10.5194/HESS-16-2585-2012.
- Wehrhan, Marc; Rauneker, Philipp; Sommer, Michael (2016): UAV-Based Estimation of Carbon Exports from  
Heterogeneous Soil Landscapes--A Case Study from the CarboZALF Experimental Area. In *Sensors (Basel, Switzerland)* 16  
(2), p. 255. DOI: 10.3390/s16020255.
- 680 Wehrhan, Marc; Sommer, Michael (2021): A Parsimonious Approach to Estimate Soil Organic Carbon Applying Unmanned  
Aerial System (UAS) Multispectral Imagery and the Topographic Position Index in a Heterogeneous Soil Landscape. In  
*Remote Sensing* 13 (18), p. 3557. DOI: 10.3390/rs13183557.
- Wessolek, Gerd; Asseng, Senthold (2006): Trade-off between wheat yield and drainage under current and climate change  
conditions in northeast Germany. In *European Journal of Agronomy* 24 (4), pp. 333–342. DOI: 10.1016/j.eja.2005.11.001.
- 685 Wilken, Florian; Ketterer, Michael; Koszinski, Sylvia; Sommer, Michael; Fiener, Peter (2020): Understanding the role of  
water and tillage erosion from <sup>239+240</sup>Pu tracer measurements using inverse modelling. In *SOIL* 6 (2), pp. 549–564. DOI:  
10.5194/soil-6-549-2020.
- WRB (2014): International soil classification system for naming soils and creating legends for soil maps. World Soil  
Resources Reports No. 106: Food and Agriculture Organization of the United Nations Rome, Italy.
- 690 Xu, Tongren; Guo, Zhixia; Liu, Shaomin; He, Xinlei; Meng, Yangfanyu; Xu, Ziwei et al. (2018): Evaluating Different  
Machine Learning Methods for Upscaling Evapotranspiration from Flux Towers to the Regional Scale. In *JGR Atmospheres*  
123 (16), pp. 8674–8690. DOI: 10.1029/2018JD028447.

695

700



705

Tables:

710

**Table 1:** Statistical values for the calibration of all gap-filling approaches and treatments.

Approach	MAE	NRMSE	NSE	R2	Approach	MAE	NRMSE	NSE	R2
<b>RG-ca nm</b>					<b>RG-ca m</b>				
<b>MDV</b>	0.26	39.2	0.85	0.85	<b>MDV</b>	0.24	35.4	0.87	0.88
<b>LUT</b>	0.06	11.5	0.99	0.99	<b>LUT</b>	0.06	11.9	0.99	0.99
<b>NLR</b>	0.51	50.7	0.74	0.75	<b>NLR</b>	0.49	48.6	0.76	0.77
<b>SVM</b>	0.26	30	0.91	0.91	<b>SVM</b>	0.24	28.7	0.92	0.92
<b>ANN_BR</b>	0.28	28.1	0.92	0.92	<b>ANN_BR</b>	0.24	25.5	0.93	0.93
<b>LL-ng nm</b>					<b>LL-ng m</b>				
<b>MDV</b>	0.25	28.7	0.92	0.92	<b>MDV</b>	0.24	29.7	0.91	0.91
<b>LUT</b>	0.06	10.9	0.99	0.99	<b>LUT</b>	0.06	10.7	0.99	0.99
<b>NLR</b>	0.48	41.6	0.83	0.83	<b>NLR</b>	0.49	41.3	0.83	0.84
<b>SVM</b>	0.25	23.1	0.95	0.95	<b>SVM</b>	0.26	24.1	0.94	0.94
<b>ANN_BR</b>	0.28	24.5	0.94	0.94	<b>ANN_BR</b>	0.27	24.3	0.94	0.94
<b>LL-cv nm</b>					<b>LL-cv m</b>				
<b>MDV</b>	0.22	30.4	0.91	0.91	<b>MDV</b>	0.21	29.1	0.92	0.92
<b>LUT</b>	0.06	13.3	0.98	0.98	<b>LUT</b>	0.05	10.9	0.99	0.99
<b>NLR</b>	0.44	42	0.82	0.83	<b>NLR</b>	0.43	41.8	0.83	0.83
<b>SVM</b>	0.23	25.1	0.94	0.94	<b>SVM</b>	0.21	23.7	0.94	0.94
<b>ANN_BR</b>	0.26	26.8	0.93	0.93	<b>ANN_BR</b>	0.25	26.5	0.93	0.93

715

720

725

730

735





**Table 2:** Statistical values for the validation of all gap-filling approaches and treatments.

Approach	MAE	NRMSE	NSE	R2	Approach	MAE	NRMSE	NSE	R2
<b>RG-ca nm</b>					<b>RG-ca m</b>				
<b>MDV</b>	0.27	44.5	0.8	0.82	<b>MDV</b>	0.23	35.4	0.87	0.88
<b>LUT</b>	0.69	72.3	0.48	0.48	<b>LUT</b>	0.65	71.1	0.49	0.5
<b>NLR</b>	0.51	50.9	0.74	0.75	<b>NLR</b>	0.49	48.8	0.76	0.77
<b>SVM</b>	0.3	33.9	0.89	0.89	<b>SVM</b>	0.28	32	0.9	0.9
<b>ANN_BR</b>	0.31	32.1	0.9	0.9	<b>ANN_BR</b>	0.27	29.6	0.91	0.91
<b>LL-ng nm</b>					<b>LL-ng m</b>				
<b>MDV</b>	0.25	31	0.9	0.91	<b>MDV</b>	0.25	31.6	0.9	0.9
<b>LUT</b>	0.74	65.9	0.57	0.57	<b>LUT</b>	0.78	67.7	0.54	0.54
<b>NLR</b>	0.48	41.7	0.83	0.83	<b>NLR</b>	0.49	41.4	0.83	0.84
<b>SVM</b>	0.28	25.4	0.94	0.94	<b>SVM</b>	0.29	26.6	0.93	0.93
<b>ANN_BR</b>	0.3	26.2	0.93	0.93	<b>ANN_BR</b>	0.29	26.3	0.93	0.93
<b>LL-cv nm</b>					<b>LL-cv m</b>				
<b>MDV</b>	0.24	33.7	0.89	0.89	<b>MDV</b>	0.21	30.3	0.91	0.91
<b>LUT</b>	0.72	72.3	0.48	0.48	<b>LUT</b>	0.65	68.8	0.53	0.53
<b>NLR</b>	0.44	42.2	0.82	0.83	<b>NLR</b>	0.43	42	0.82	0.83
<b>SVM</b>	0.26	28.2	0.92	0.92	<b>SVM</b>	0.23	26.3	0.93	0.93
<b>ANN_BR</b>	0.28	29.8	0.91	0.91	<b>ANN_BR</b>	0.28	29.5	0.91	0.91

740

745

750

755

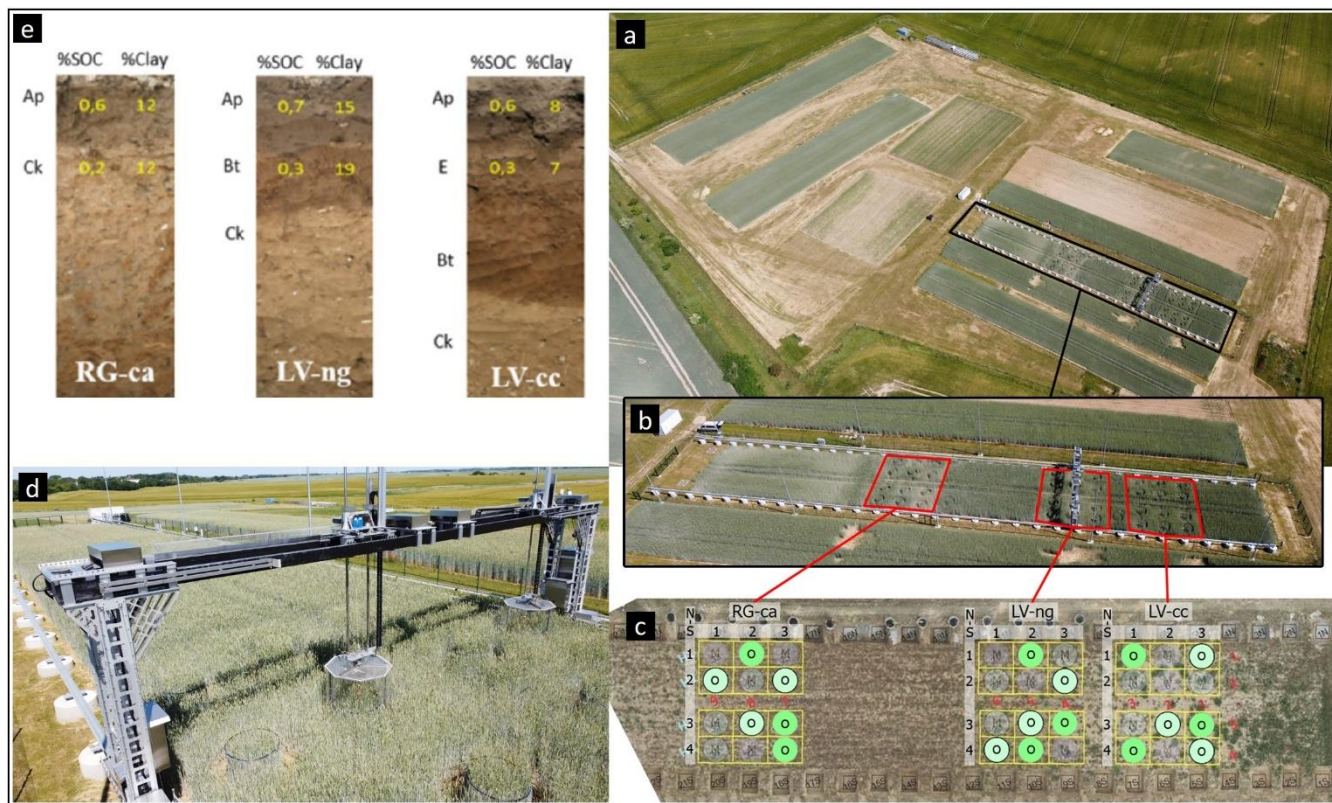
760

765

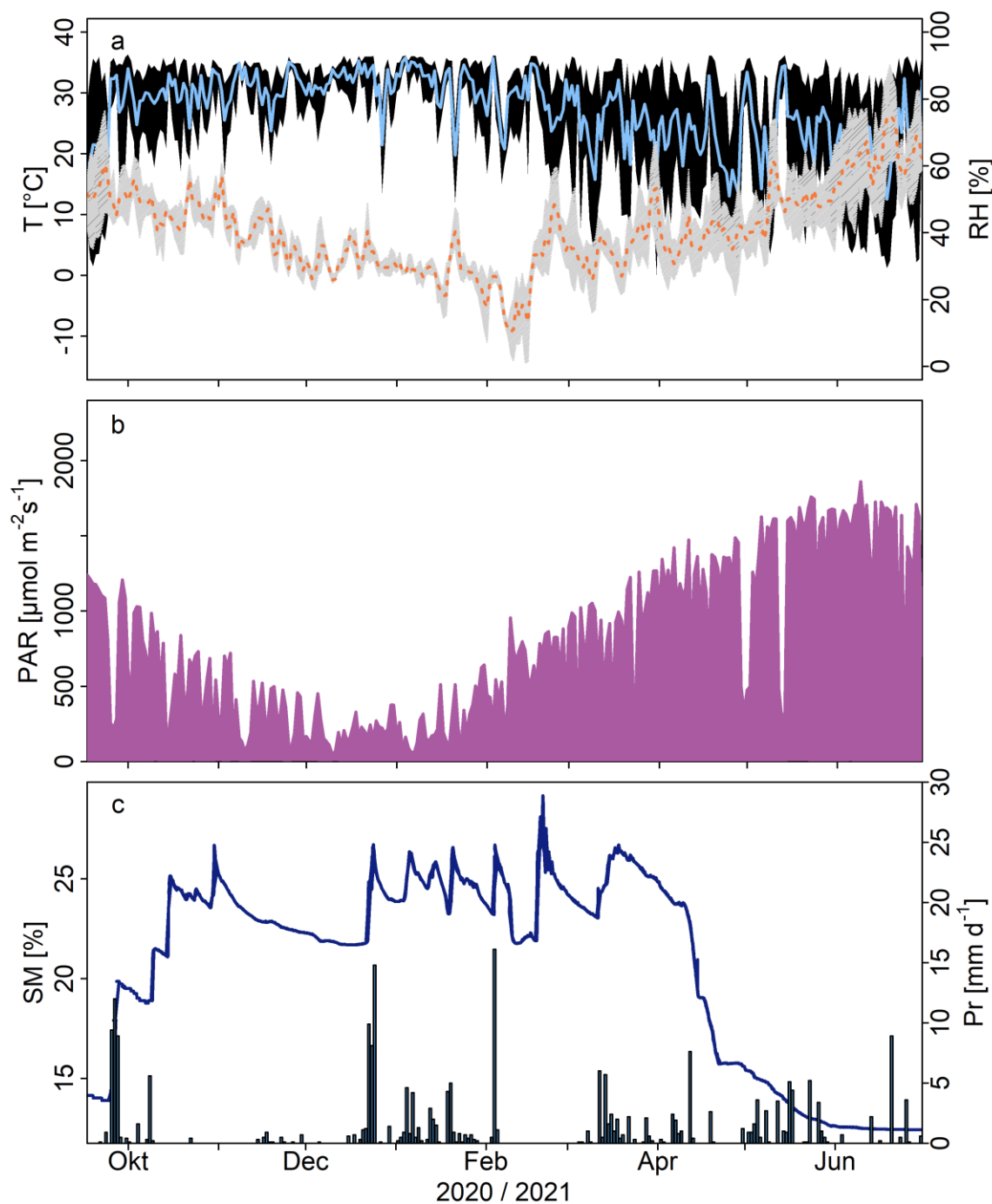


770

Figures:

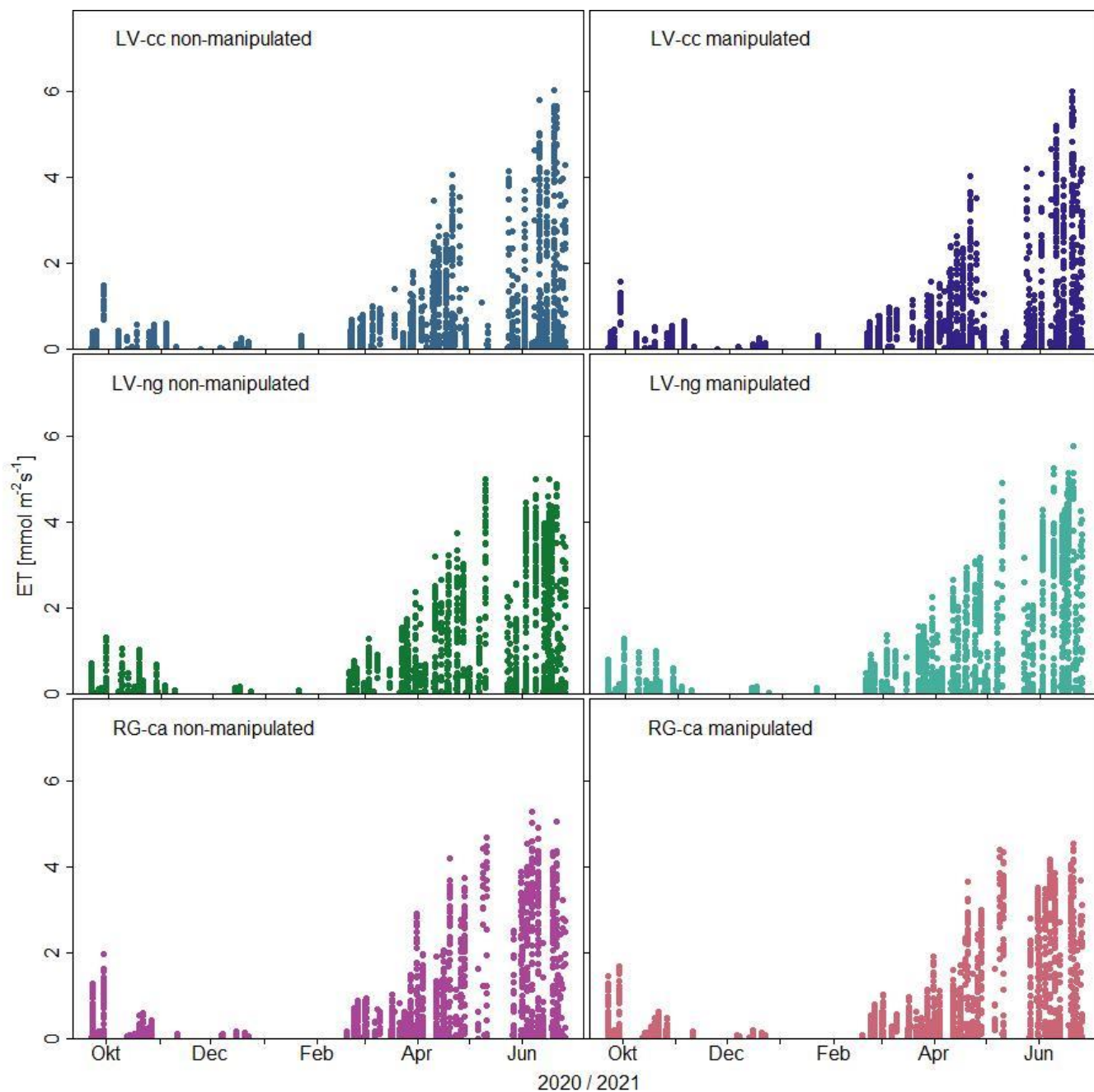


775 **Figure 1:** (a) AgroFLUX research site in the CarboZALF-D experimental area with (b) the 110 x 16 m field where (d) the FluxCrane operates on (c) 18 measurement plots from (e) three different soil types (LV-cc: non-eroded calcareous Luvisol, LV-ng: highly eroded nudiargic Luvisol, and RG-ca: extremely eroded calcareous Regosol).

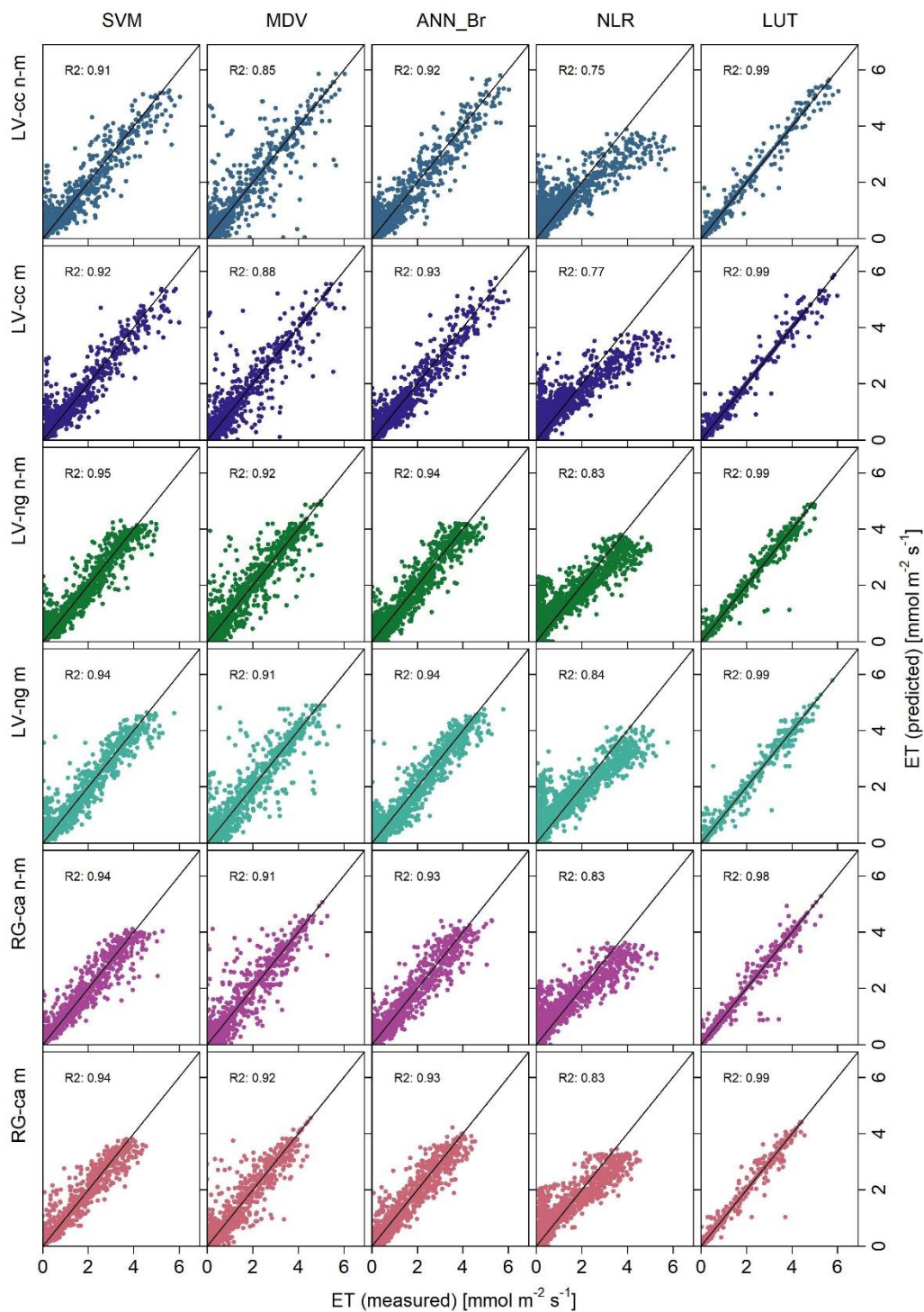


780

**Figure 2:** Environmental parameters during the measurement period with (a) daily mean temperatures (orange line; light grey = associated variation) and daily mean relative humidity (black line; dotted lines = associated variation), (b) photosynthetically active radiation (purple) and (c) soil moisture (blue line) and precipitation (blue bars).

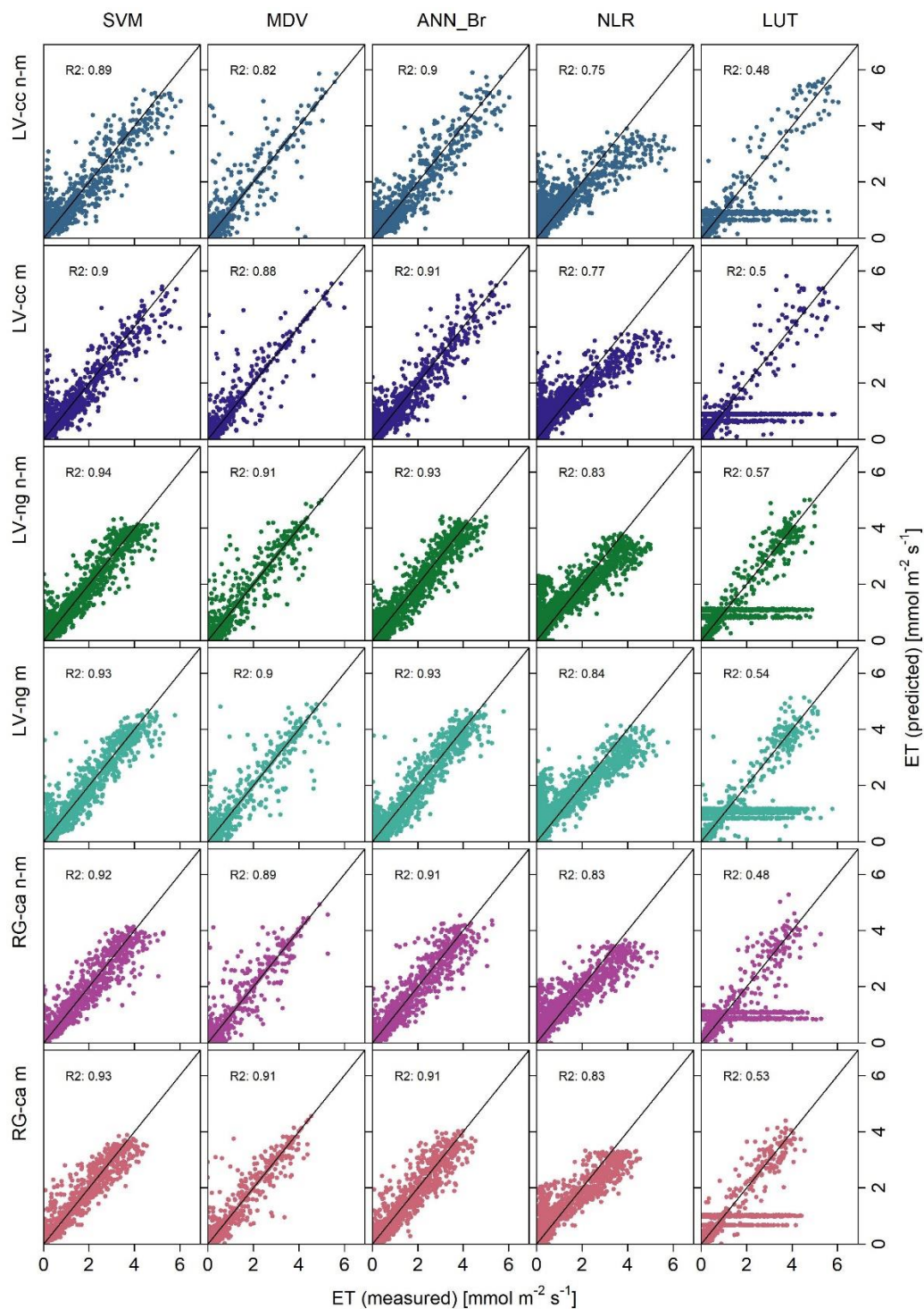


785 **Figure 3:** Measured ET fluxes of the three soil types (replicates summarized) over the entire observation period (non-manipulated treatments on the left, manipulated treatments on the right).



790

**Figure 4:** Comparison of the measured (bottom) with the predicted (left) ET fluxes and associated r-square values (R2) of the calibration results of all approaches. The black line forms the 1/1 line. The different treatments are shown above, the approaches on the right.



795 **Figure 5:** Comparison of the measured (bottom) with the predicted (left) ET fluxes and associated r-square values (R2) of the validation results of all approaches. The black line forms the 1/1 line. The different treatments are shown above, the approaches on the right.

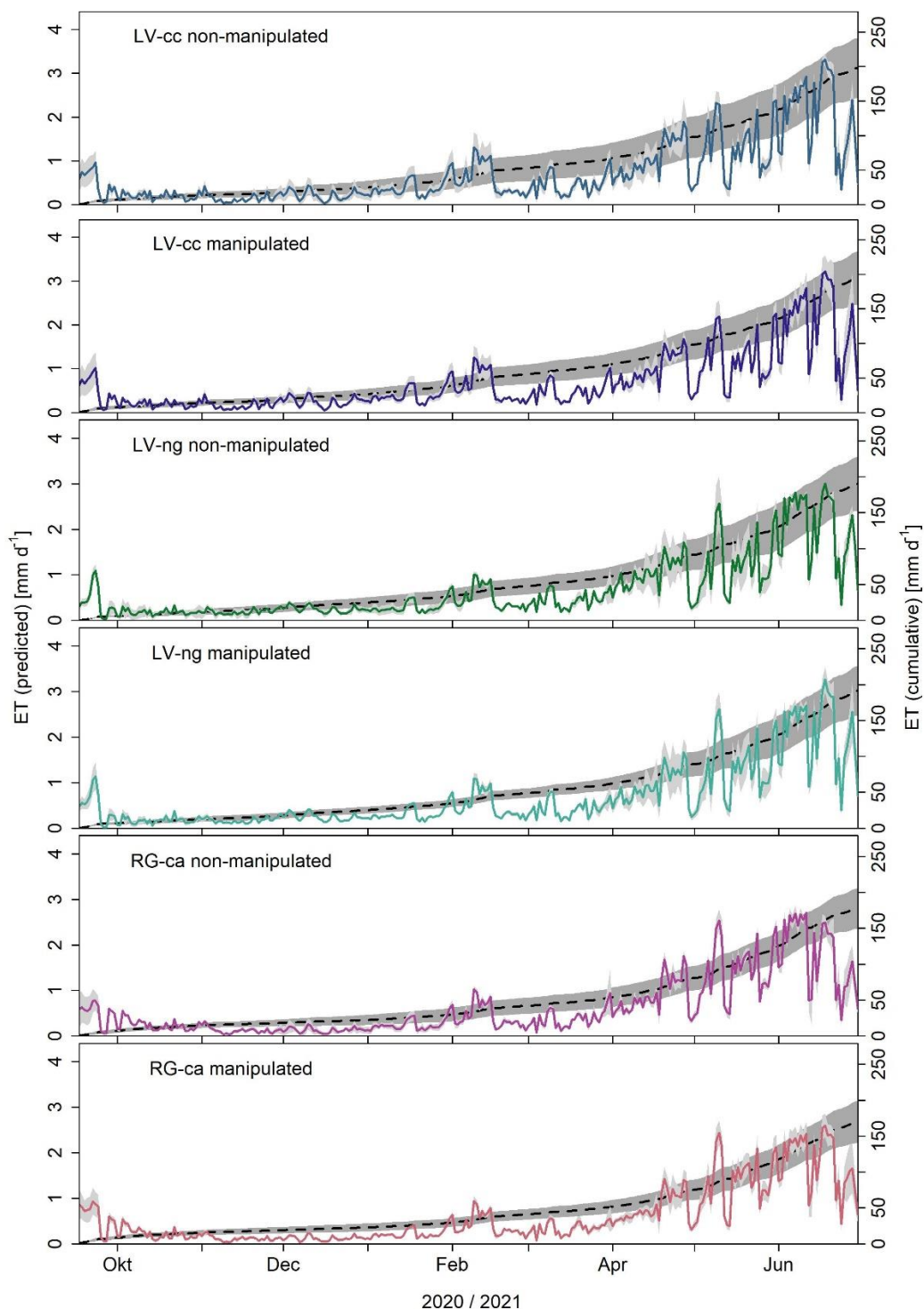
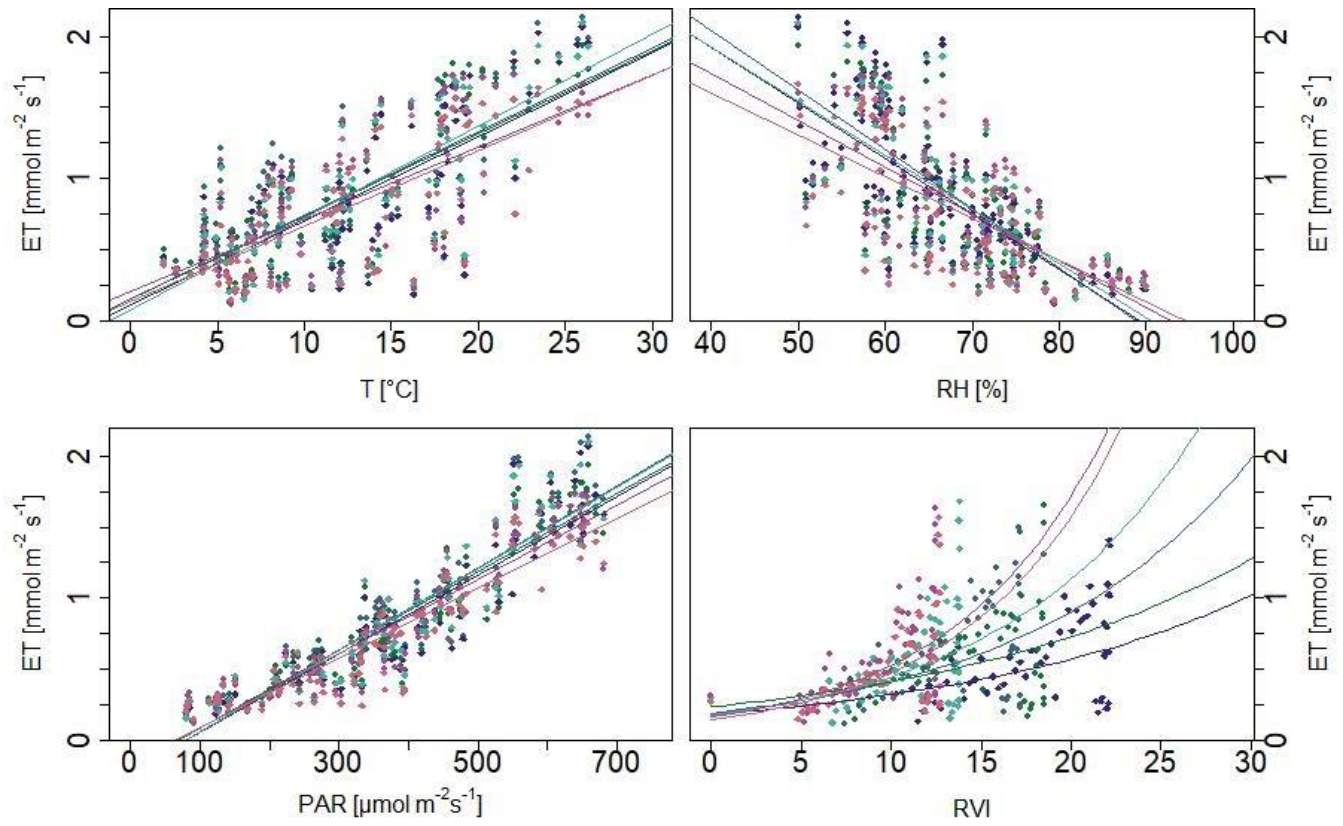


**Figure 6:** Daily mean ET sums (colored lines) of the different treatments and mean seasonal ET budgets (dashed lines) with variations between replicates (light and dark grey).



800 **Figure 7:** Relationship between ET and temperature (T) [°C], relative humidity (rH) [%], photosynthetically active radiation (PAR) [μmol m<sup>-2</sup> s<sup>-1</sup>] and ratio vegetation index (RVI) [mmol m<sup>-2</sup> s<sup>-1</sup>] as well as associated regression lines.



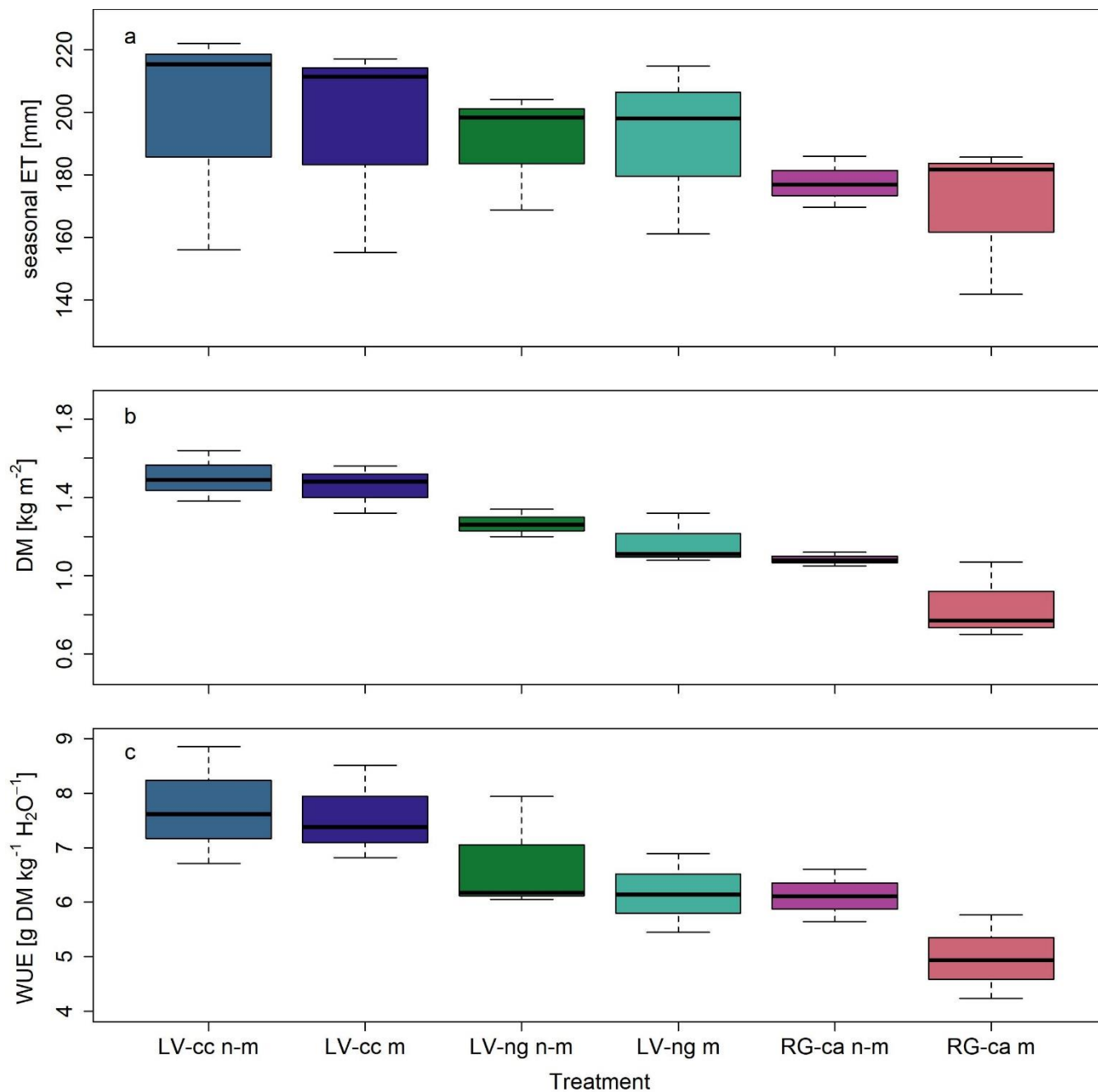
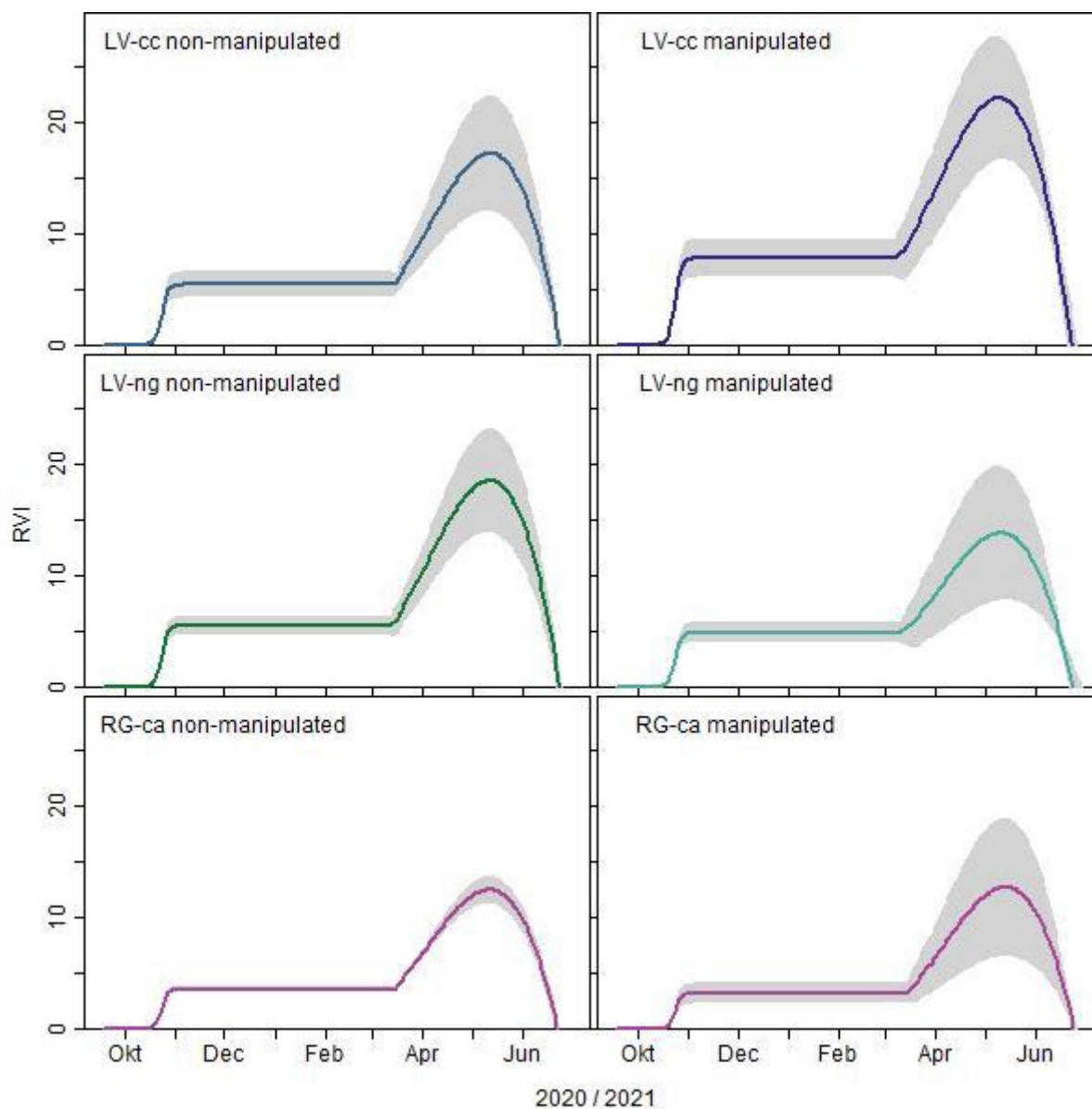


**Figure 8:** Averaged seasonal ET-totals [mm] (a), harvest in form of dry mass (DM) [kg] (b), and WUE<sub>agro</sub> of the different treatments and the associated standard deviation.



Appendix A:



810

**Figure A1:** RVI fit (colored lines) of the different treatments with variations between replicates (light grey).

815

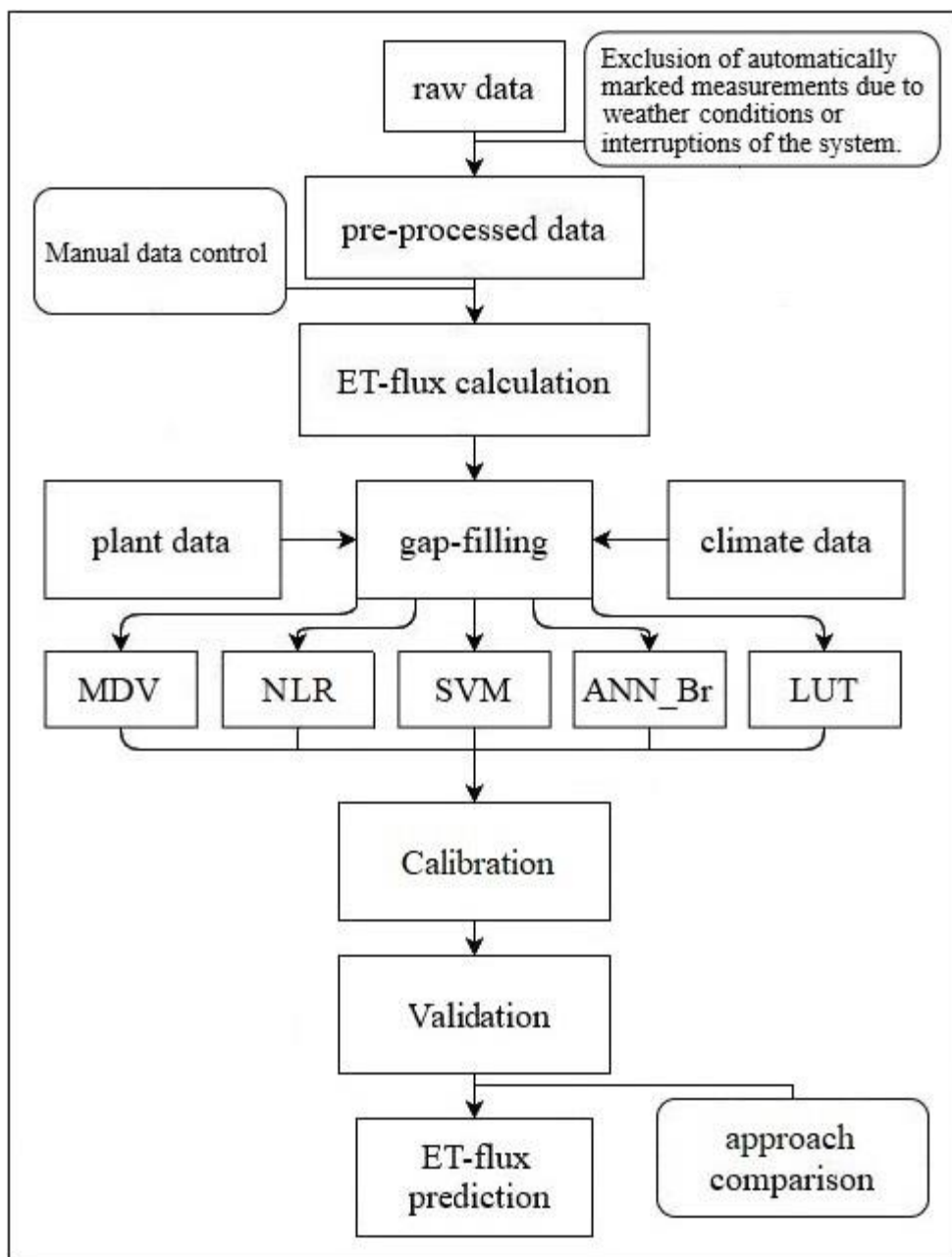


**Figure A2:** Schematic representation of the main steps of the presented data processing: raw data preparation was followed by a campaign-specific ET-flux calculation. Then, environmental parameters were used for gap filling using five different approaches. After calibration and validation, the most accurate approach was used for gap filling.



## Appendix B:

**Table B1:** Used R packages and associated sources.

	<b>package</b>	<b>source</b>
825	Akima	Akima & Gebhardt (2021)
	Andrews	Myslivec (2012)
	Base	R Core Team (2021)
	Boot	Davison & Hinkley (1997)
830	Caret	Kuhn (2021)
	data.table	Dowle & Srinivasan (2021)
	e1071	Meyer et al. (2021)
	FSA	Ogle et al. (2022)
	ggplot2	Wickham (2016)
	gridExtra	Auguie (2017)
835	gt	Iannone et al. (2022)
	hydroGOF	Mauricio Zambrano-Bigiarini (2020)
	Kernlab	Karatzoglou et al. (2004)
	Latrrice	Sarkar (2008)
	Lmtest	Zeileis & Hothorn (2002)
	lookupTable	Jia & Maier (2015)
840	Lubridate	Grolemund & Wickham (2011)
	Neuralnet	Fritsch et al. (2019)
	Nortest	Gross & Ligges (2015)
	Plotrix	J (2006)
	Plyr	Wickham (2011)
	Reshape	Wickham (2007)
845	Shape	Soetaert (2021)
	Tibble	Müller & Wickham (2021)
	tidyr	Wickham & Girlich (2022)
	Vioplot	Adler & Kelly (2020)
	webshot	Chang (2022)
850	Zoo	Zeileis & Grothendieck (2005)

855



**Table B2:** Statistical values ( $r^2$  and  $p$ ) for the relationship between ET and response variables (environmental parameter).

Treatment	Parameter	$r^2$	$p$
LV-cc n-m	T	0.49	4.27E-16
LV-cc m	T	0.54	3.52E-18
LV-ng n-m	T	0.54	3.02E-18
LV-ng m	T	0.61	7.71E-22
RG-ca n-m	T	0.46	1.05E-14
RG-ca m	T	0.56	3.45E-19
LV-cc n-m	RH	0.56	1.71E-19
LV-cc m	RH	0.54	3.10E-18
LV-ng n-m	RH	0.52	1.57E-17
LV-ng m	RH	0.48	1.48E-15
RG-ca n-m	RH	0.44	5.30E-14
RG-ca m	RH	0.39	4.11E-12
LV-cc n-m	PAR	0.84	1.40E-41
LV-cc m	PAR	0.84	2.12E-41
LV-ng n-m	PAR	0.85	3.82E-43
LV-ng m	PAR	0.85	4.43E-43
RG-ca n-m	PAR	0.87	3.57E-45
RG-ca m	PAR	0.85	6.75E-43
LV-cc n-m	RVI	0.24	1.67E-04
LV-cc m	RVI	0.2	6.51E-04
LV-ng n-m	RVI	0.17	1.76E-03
LV-ng m	RVI	0.21	4.81E-04
RG-ca n-m	RVI	0.33	5.06E-06
RG-ca m	RVI	0.39	3.47E-07

860

865

870

875

880

885

890